Status of CMD-3 experiment at Novosibirsk

Ivan Logashenko (BINP)

on behalf of CMD-3 collaboration

The 5th Plenary Workshop of the Muon g-2 Theory Initiative

University of Edinburgh

September 5-9, 2022

VEPP-2000

250 m beamline

VEPP-2000

Injection complex (2017-)

Round beam optics

Energy monitoring by Compton backscattering ($\sigma_{\sqrt{s}} \approx 0.1$ MeV)

Design parameters @ 1 GeV	
Circumference	24.388 m
Beam energy	150 ÷ 1000 MeV
N of bunches	1×1
N of particles	1×10^{11}
Betatron tunes	4.14 / 2.14
Beta*	8.5 cm
BB parameter	0.1
Luminosity	1×10^{32} cm^{-2}s^{-1}

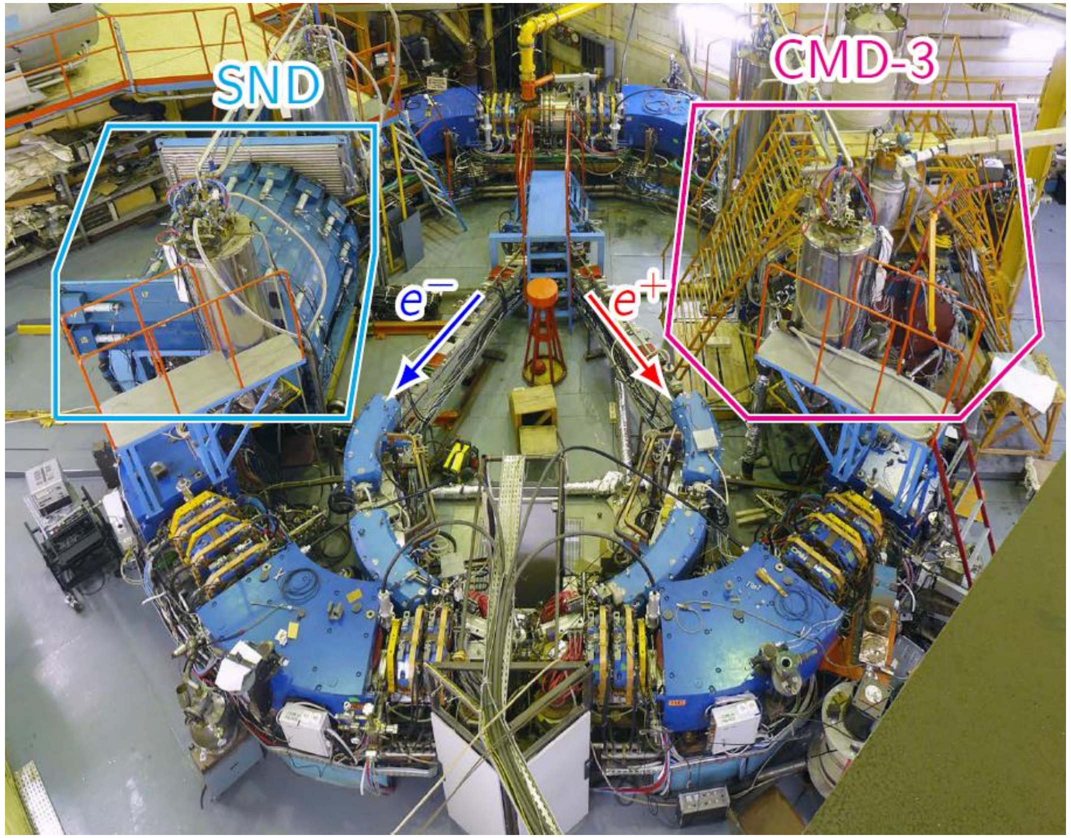

CMD-3 collected data

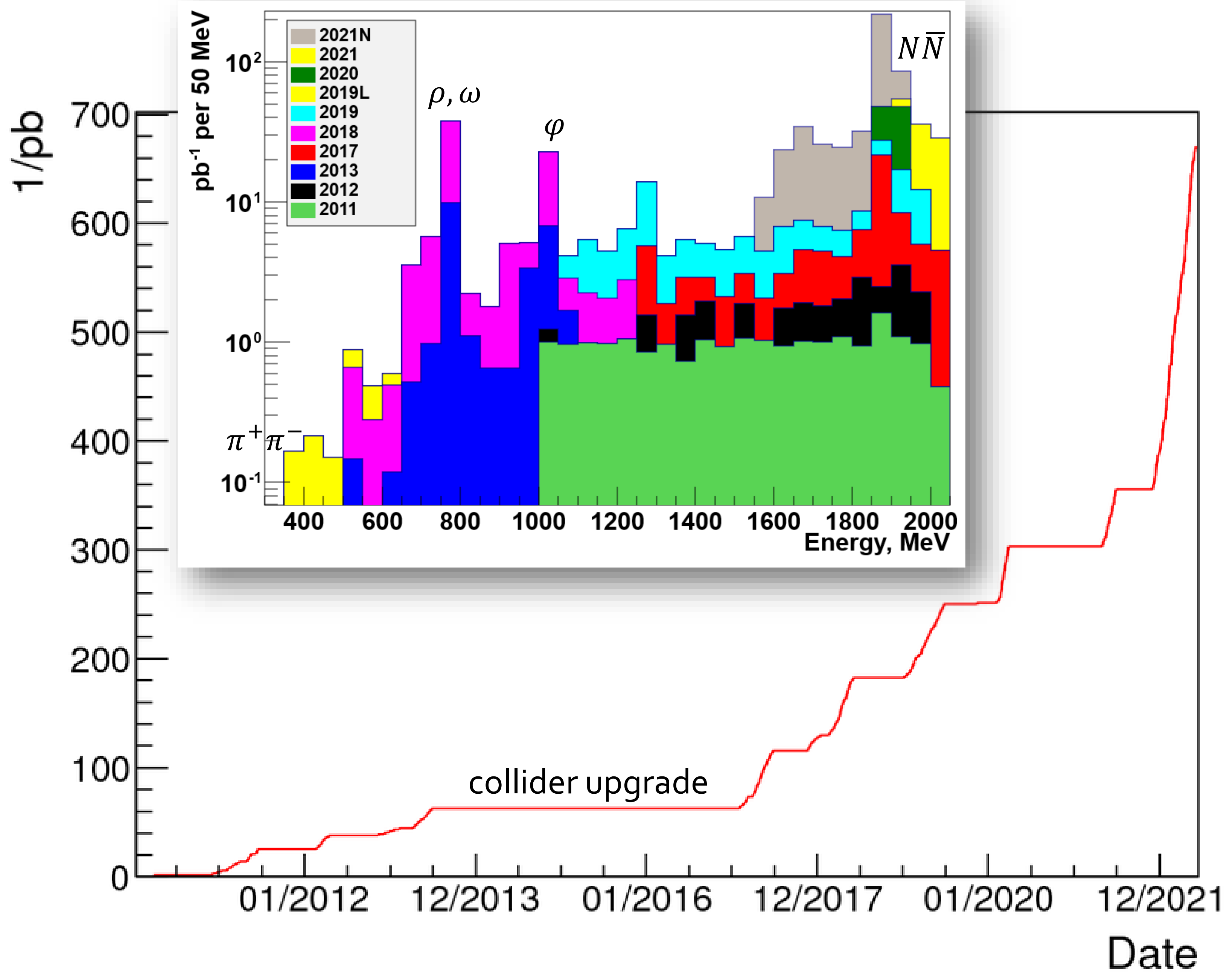

CMD-3 detector

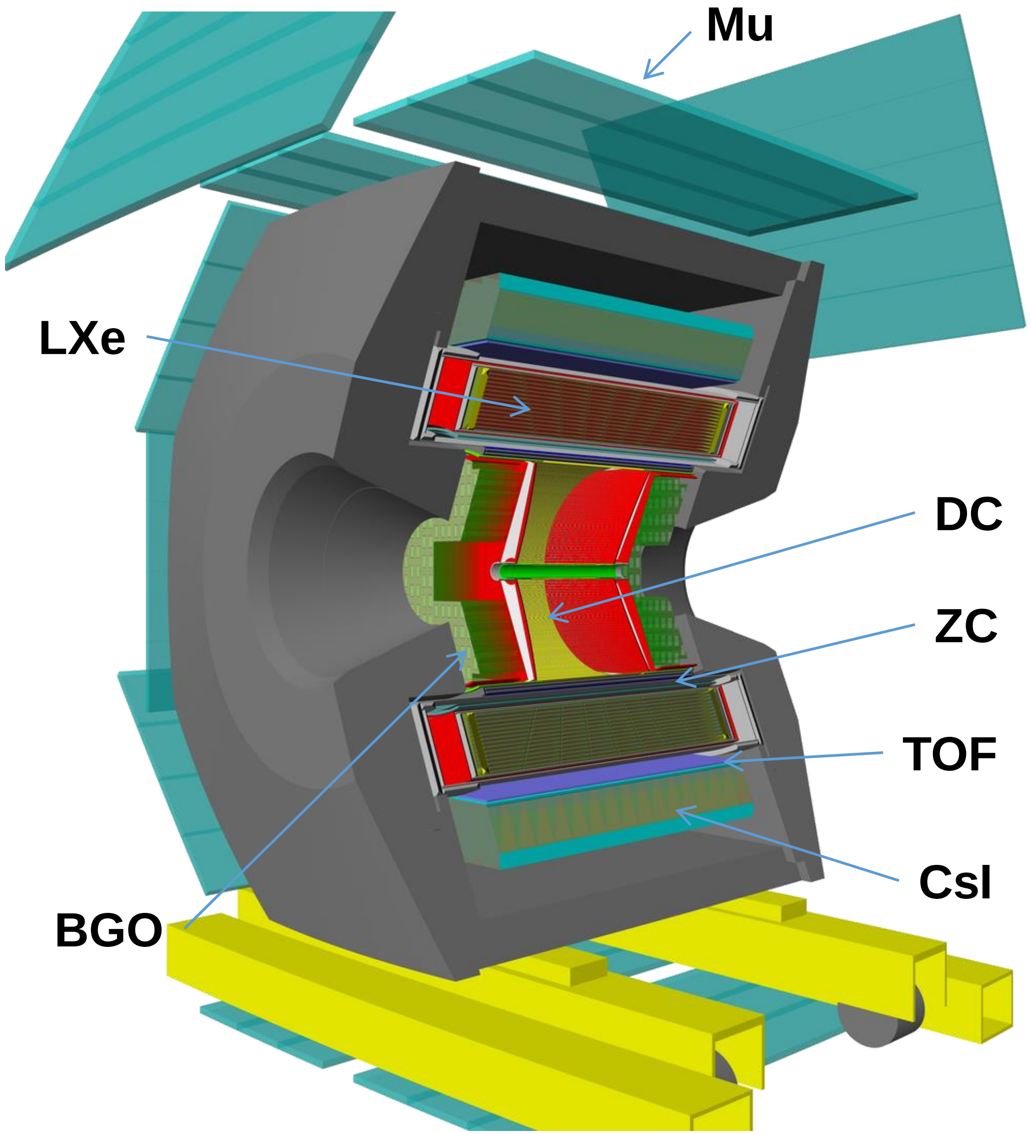

Advantages compared to CMD-2:

- new drift chamber with two times better resolution, higher B field
  - better tracking
  - better momentum resolution
- thicker barrel calorimeter ($8.3X_0 \rightarrow 13.4\ X_0$)
  - better particle separation
- LXe calorimeter
  - measurement of conversion point for γ's
  - measurement of shower profile
- TOF system
  - particle id (mainly p, n)

CMD-3 detector

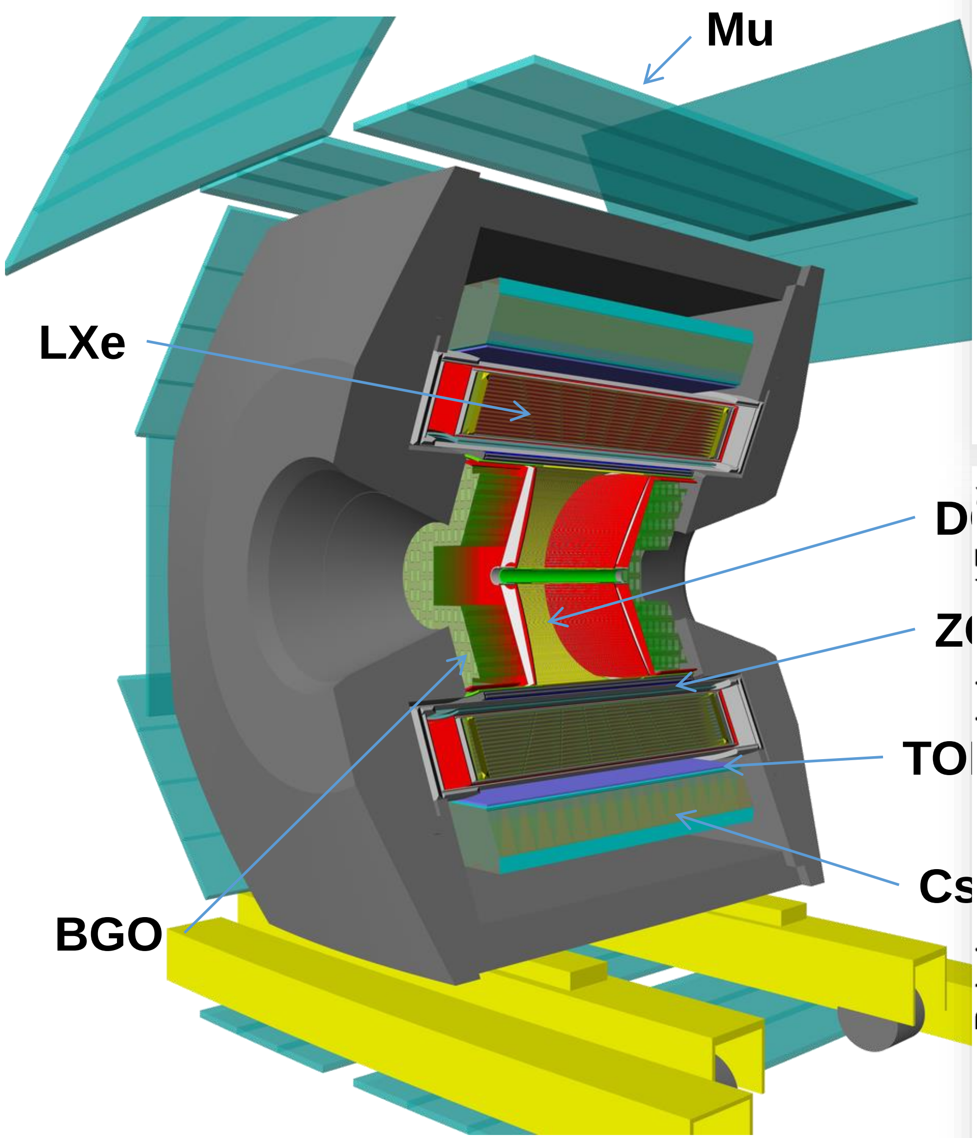

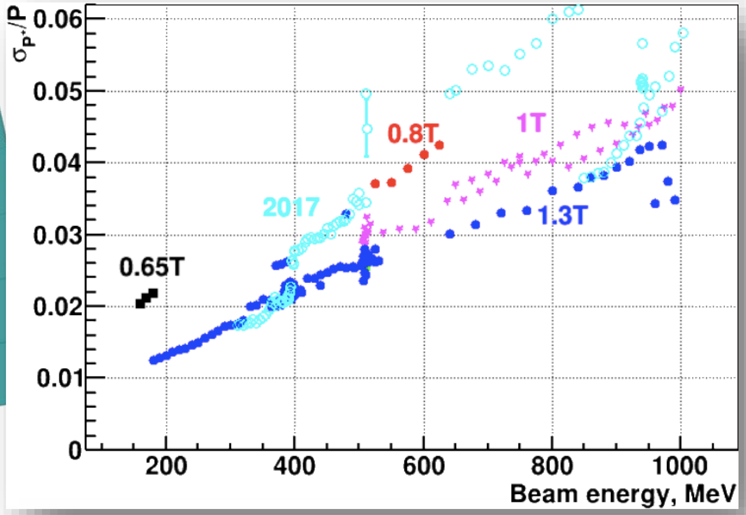

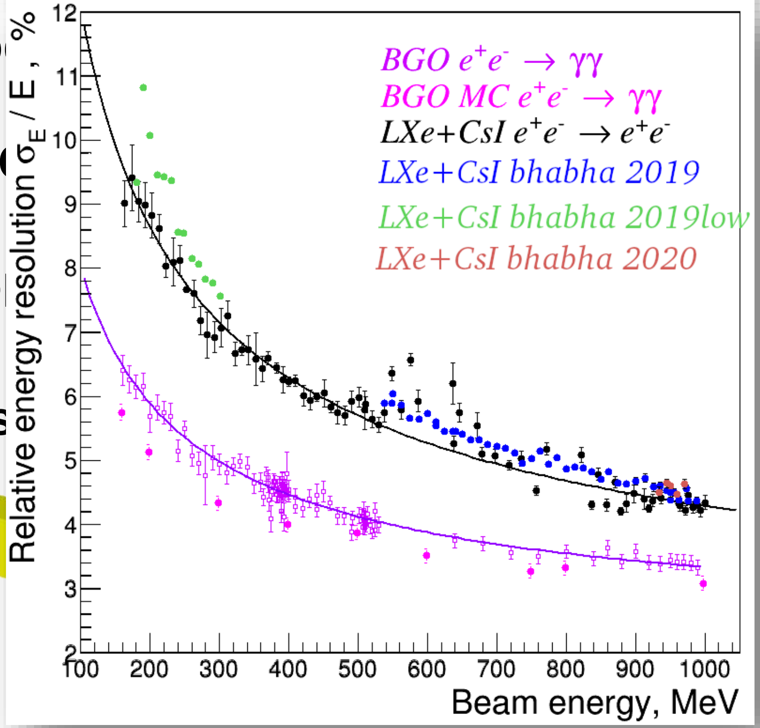

SND detector

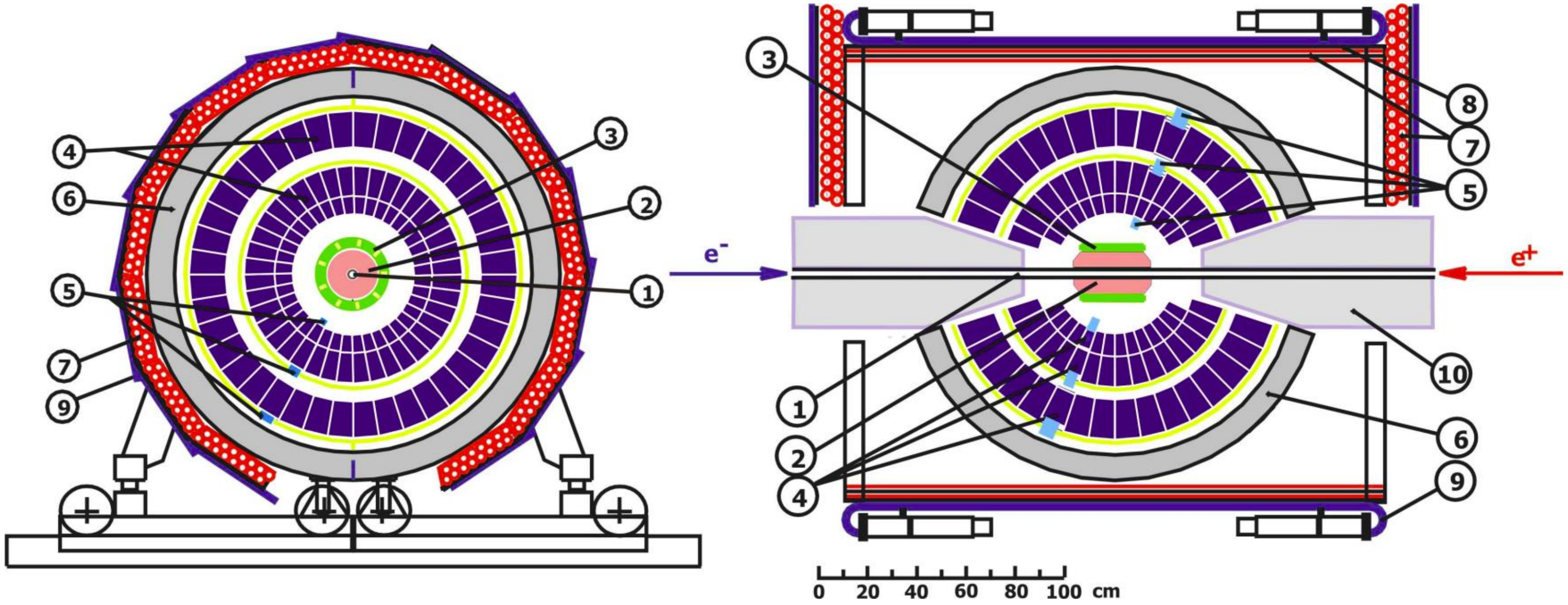

1 – beam pipe
2 – tracking system
3 – aerogel
4 – NaI(Tl) crystals
5 – phototriodes
6 – muon absorber
7–9 – muon detector
10 – focusing solenoid

Advantages compared to previous SND:

- new system - Cherenkov counter (n=1.05, 1.13)
  - e/π separation E<450 MeV
  - π/K separation E<1 GeV
- new drift chamber
  - better tracking
  - better determination of solid angle

Final states under analysis

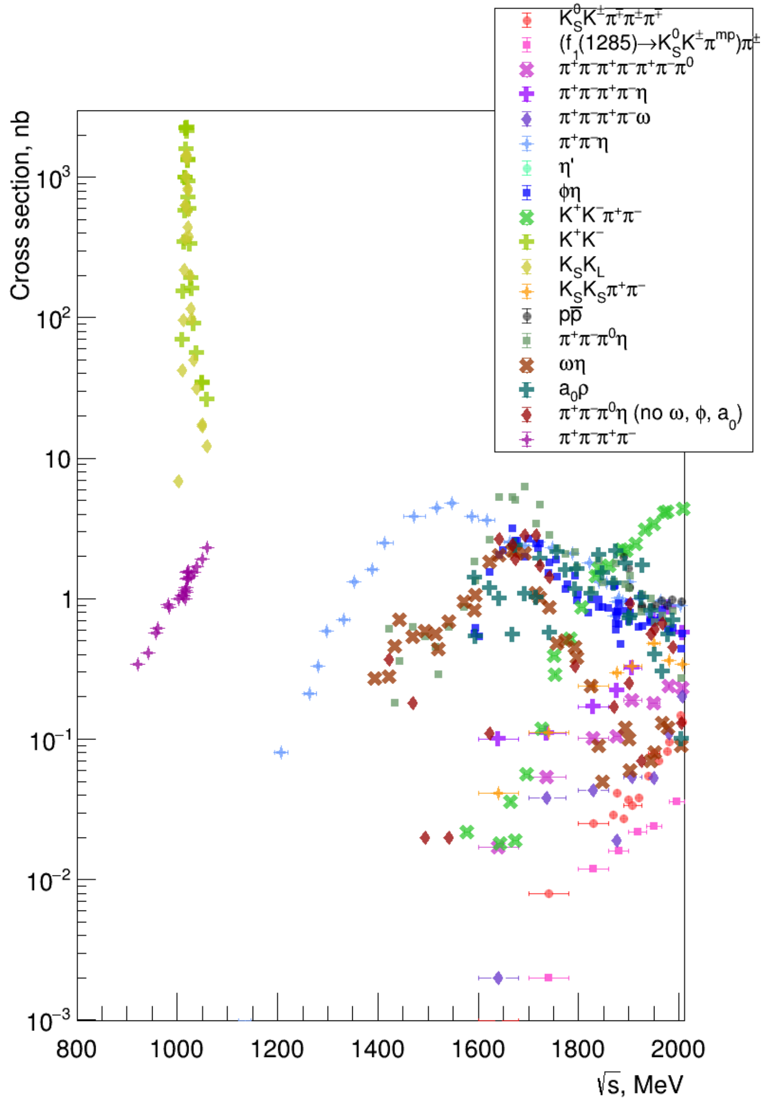

Signature	Final state (published, preliminary, under analysis or planed)
2 charged	$\pi^+\pi^-$, K^+K^-, K_SK_L, $p\bar{p}$
2 charged + γs	$\pi^+\pi^-\gamma$, $\pi^+\pi^-\pi^0$, $\pi^+\pi^-2\pi^0$, $\pi^+\pi^-3\pi^0$, $\pi^+\pi^-4\pi^0$, $\pi^+\pi^-\eta$, $\pi^+\pi^-\pi^0\eta$, $\pi^+\pi^-2\pi^0\eta$, $K^+K^-\pi^0$, $K^+K^-2\pi^0$, $K^+K^-\eta$, $K_SK_L\pi^0$, $K_SK_L\eta$
4 charged	$2(\pi^+\pi^-)$, $K^+K^-\pi^+\pi^-$, $K_SK^{\pm}\pi^{\mp}$
4 charged + γs	$2(\pi^+\pi^-)\pi^0$, $2(\pi^+\pi^-\pi^0)$, $\pi^+\pi^-\eta$, $\pi^+\pi^-\omega$, $2(\pi^+\pi^-)\eta$, $K^+K^-\omega$, $K_SK^{\pm}\pi^{\mp}\pi^0$
6 charged	$3(\pi^+\pi^-)$, $K_SK_S\pi^+\pi^-$, $K_SK^+\pi^-\pi^+\pi^-$
6 charged + γs	$3(\pi^+\pi^-)\pi^0$
Neutral	$\pi^0\gamma$, $2\pi^0\gamma$, $3\pi^0\gamma$, $\eta\gamma$, $\pi^0\eta\gamma$, $2\pi^0\eta\gamma$
Other	$n\bar{n}$, $\pi^0e^+e^-$, ηe^+e^-
Rare decays	η', $D^*(2007)^0$

CMD-3 published data

2207.04615 [hep-ex]	$K_S K^{\pm}\pi^{\mp}\pi^{+}\pi^{-}$
PLB 804 (2020) 135380	$K_S K_S \pi^{+}\pi^{-}$
JHEP 01 (2020) 112	$\eta\pi^{+}\pi^{-}$
PLB 798 (2019) 134946	$K^{+}K^{-}\eta$
PLB 792 (2019) 419	$3(\pi^{+}\pi^{-})\pi^{0}$
PLB 794 (2019) 64	$N\bar{N}$ threshold
PLB 779 (2018) 64	$K^{+}K^{-}$ $@\varphi$
PLB 773 (2017) 150	$\pi^{+}\pi^{-}\pi^{0}\eta$
PLB 768 (2017) 345	$\pi^{+}\pi^{-}\pi^{+}\pi^{-}$ $@\varphi$
PLB 760 (2016) 314	$K_S K_L$ $@\varphi$
PLB 756 (2016) 153	$K^{+}K^{-}\pi^{+}\pi^{-}$
PLB 759 (2016) 634	$p\bar{p}$
PLB 740 (2015) 273	$\eta'(958)$
PLB 723 (2013) 82	$3(\pi^{+}\pi^{-})$

CMD-3 update: $\pi^+\pi^-\pi^0$

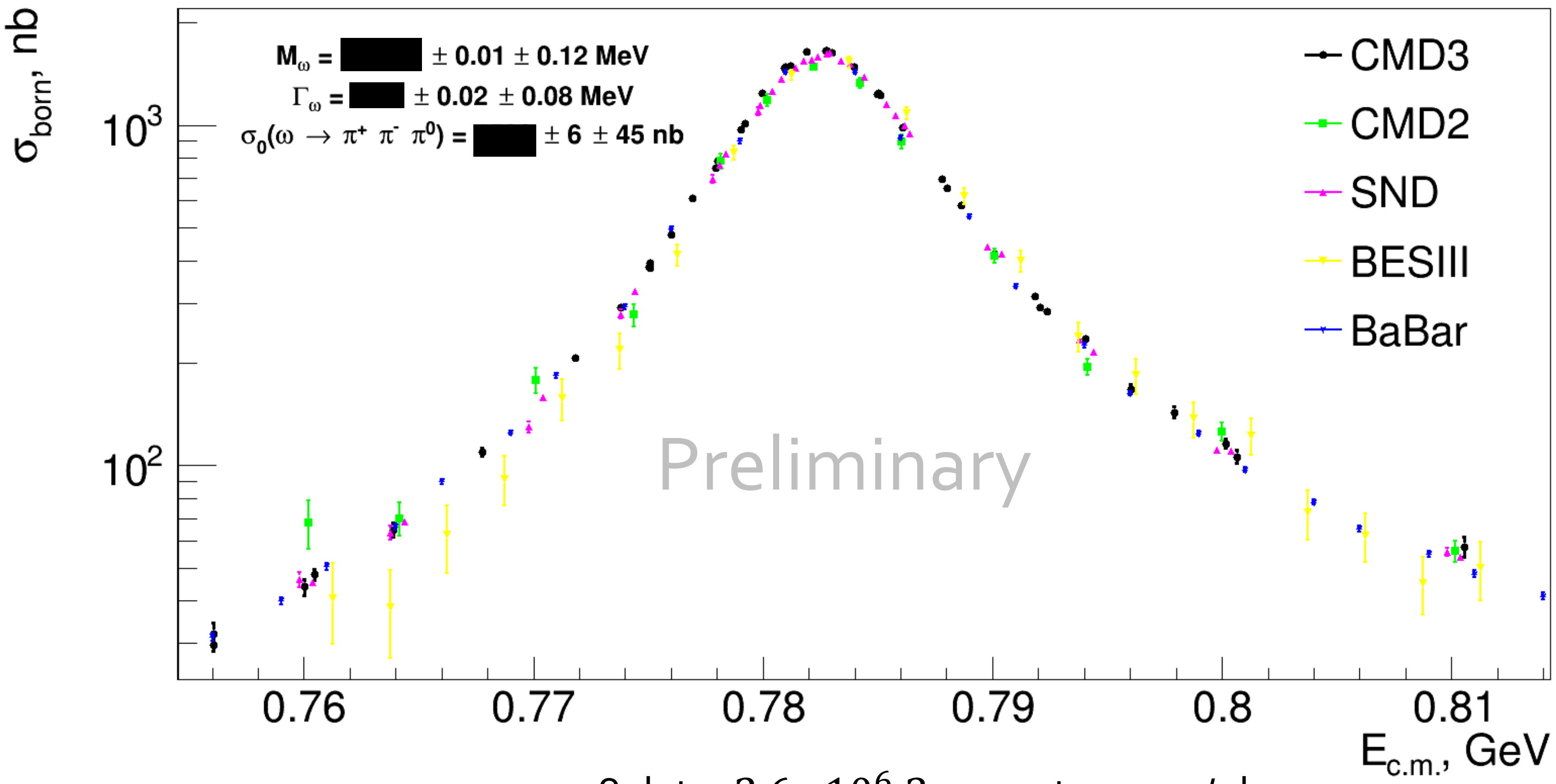

2013, 2018 data, $2.6 \cdot 10^6$ 3π events, ~54 1/pb

Results are systematics-limited

CMD-3 update: K^+K^-

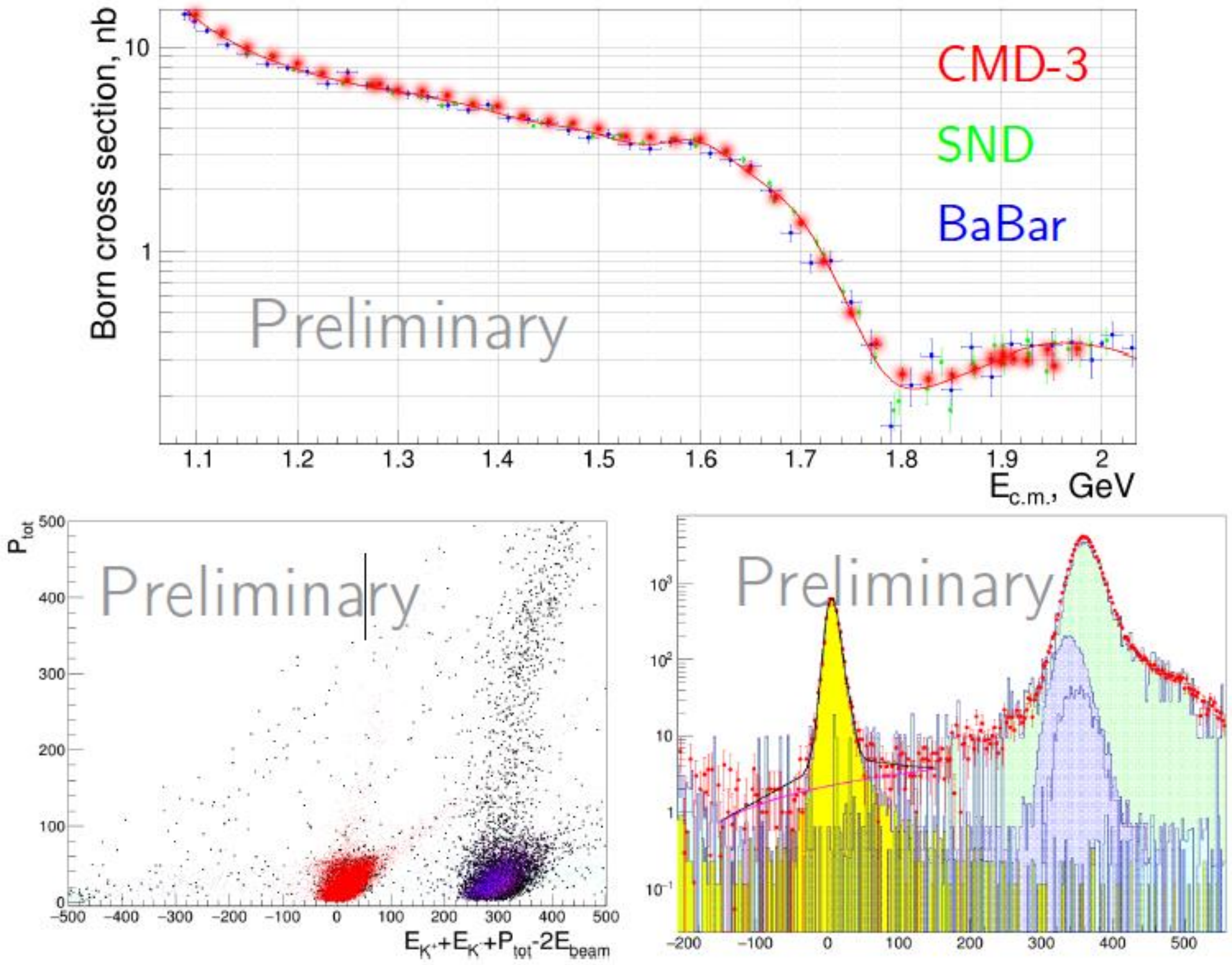

CMD-3 update: $K^+K^-\pi^0$

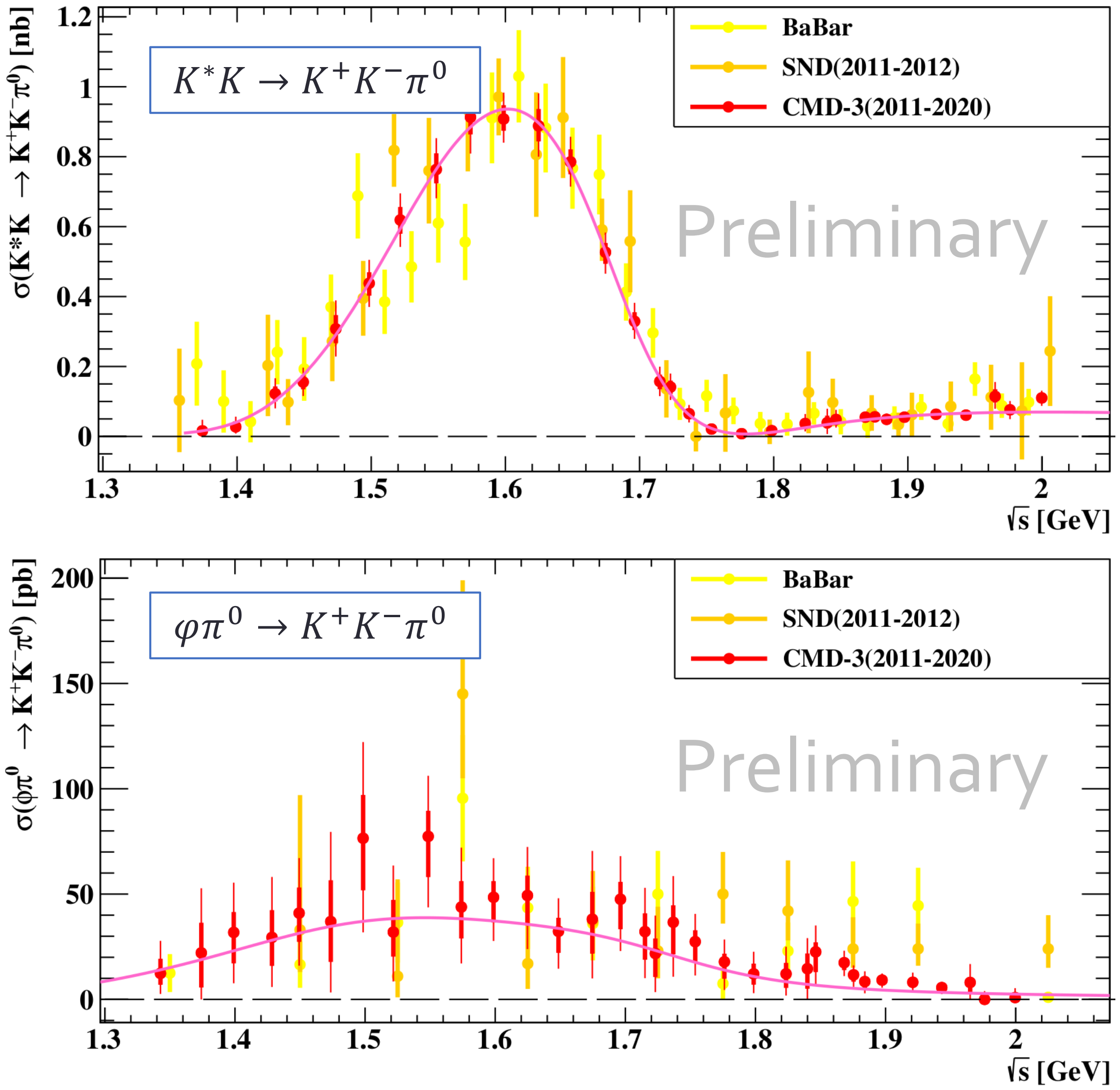

CMD-3 update:

$K_S K^{\pm}\pi^{\mp}$

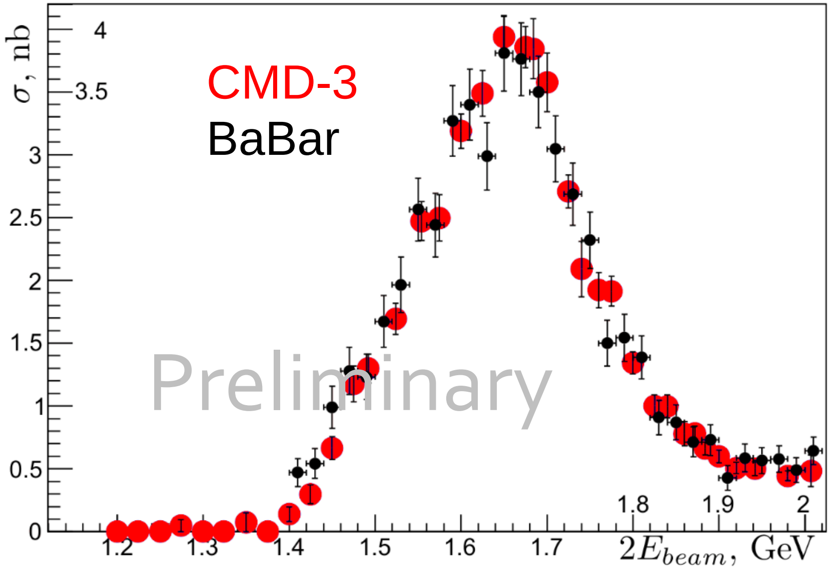

Cross section

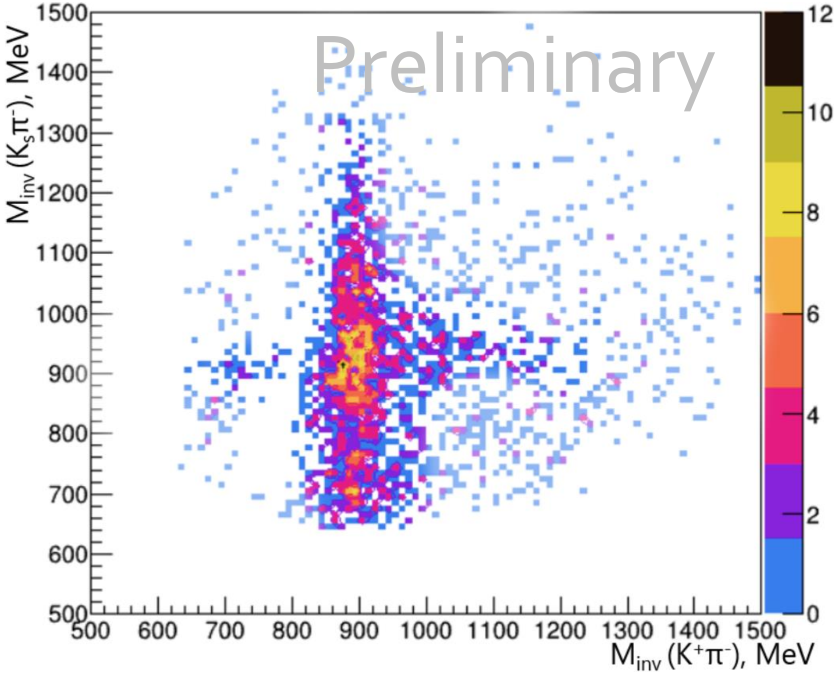

Intermediate states:
dominated by K^*K

CMD-3 update:

$K_S K^{\pm}\pi^{\mp}\pi^{+}\pi^{-}$

- Contributions from $f_1(1285)\pi^+\pi^-$, $f_1(1420)\pi^+\pi^-$ and $f_1(1510)\pi^+\pi^-$ are seen

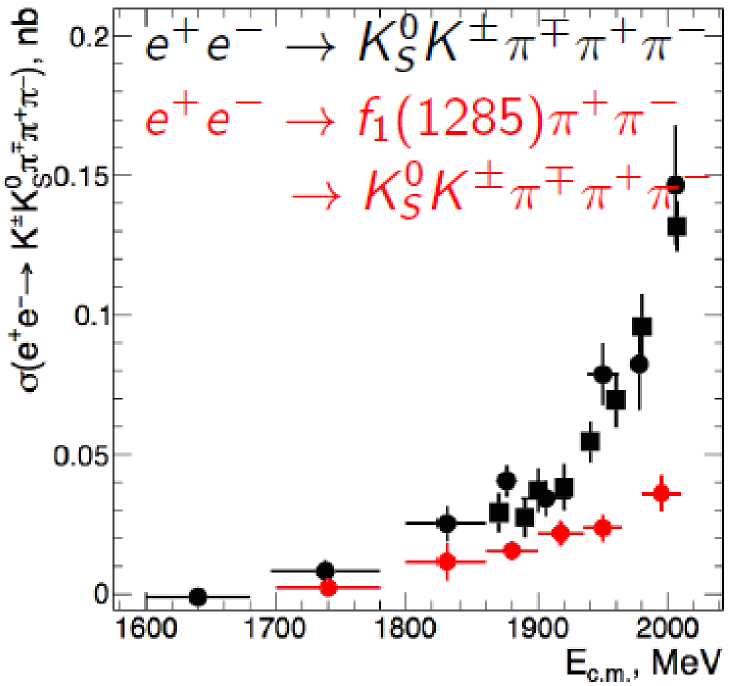

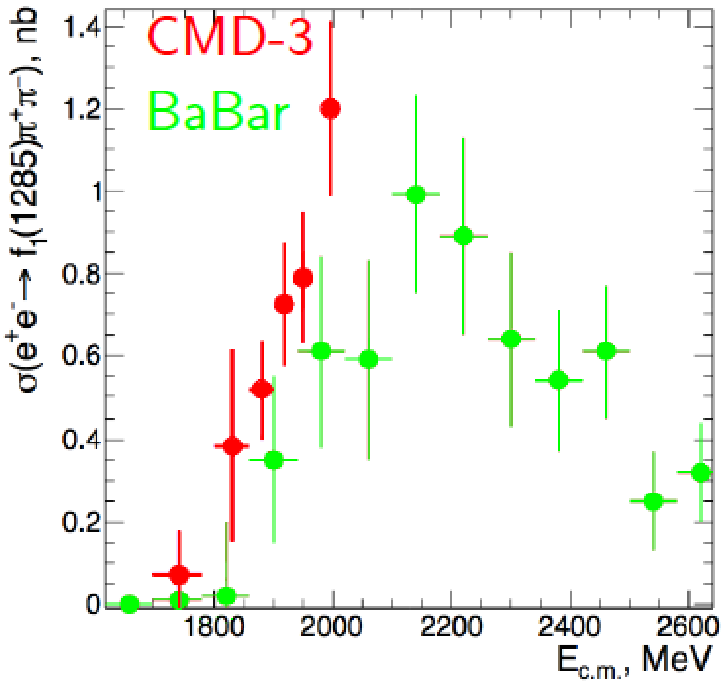

2207.04615

CMD-3 update:

$\pi^+\pi^-\pi^+\pi^-\pi^0$

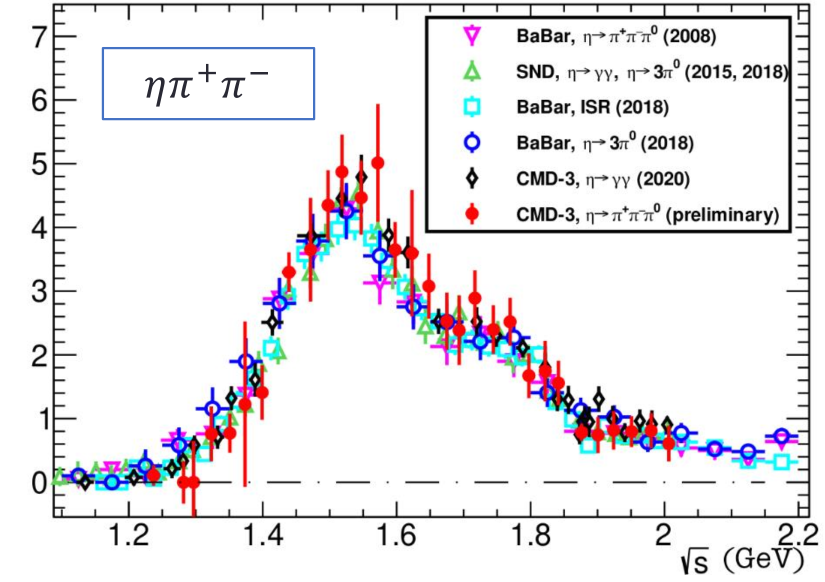

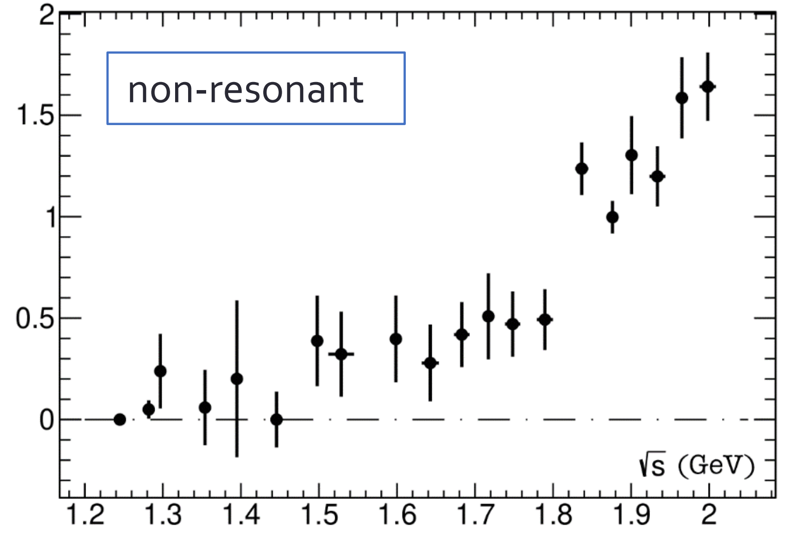

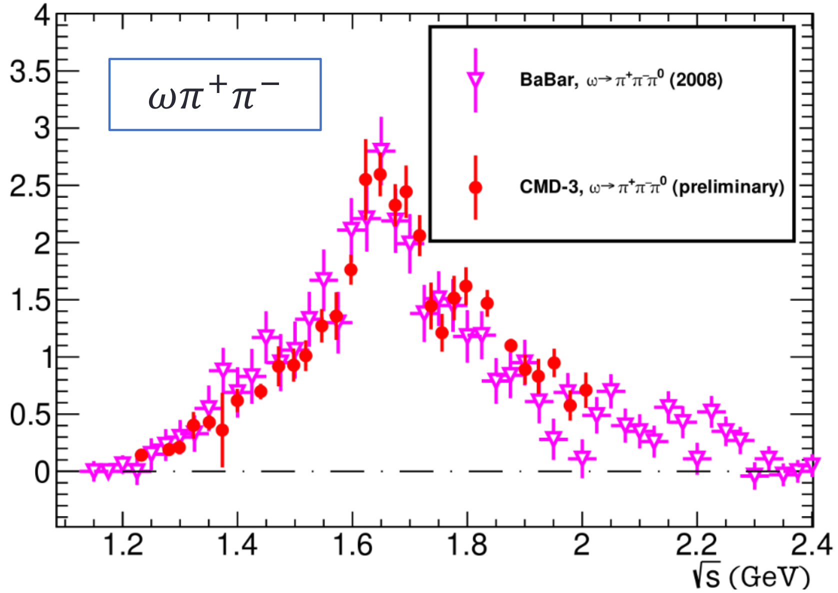

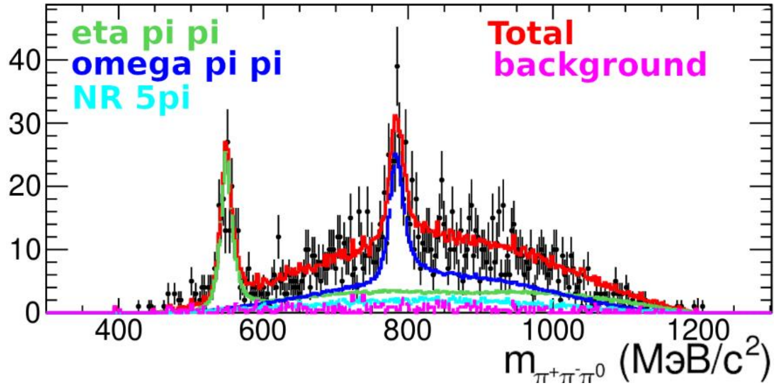

In order to measure hadronic cross section, you have to understand the dynamics of the process. **High statistics is crucial!**

Understanding of intermediate dynamics

Four pions at CMD-3

Simultaneous unbinned amplitude analysis of 150 000 $\pi^+\pi^-\pi^0\pi^0$ events and 250 000 $\pi^+\pi^-\pi^+\pi^-$ events.

Amplitudes accounted for in the likelihood function:

- $\omega[1^{--}]\pi^0[0^{++}]$ (only $\pi^+\pi^-2\pi^0$)
- $a_1(1260)[1^+]\pi[0^-]$
- $\rho[1^{--}]f^0/\sigma[0^{++}]$
- $\rho f_2(1270)[2^{++}]$
- $\rho^+\rho^-$ (only $\pi^+\pi^-2\pi^0$)
- $h_1(1170)[1^{+-}]\pi^0$ (only $\pi^+\pi^-2\pi^0$)

$$R_i(s) = \frac{\int |V_i \cdot \mathbf{H}_{i\perp}(\Omega)|^2 d\Phi}{\int |\sum_\beta V_\beta \mathbf{H}_{\beta\perp}(\Omega)|^2 d\Phi} \cdot \sigma_{2\pi^0\pi^+\pi^-}(s)$$

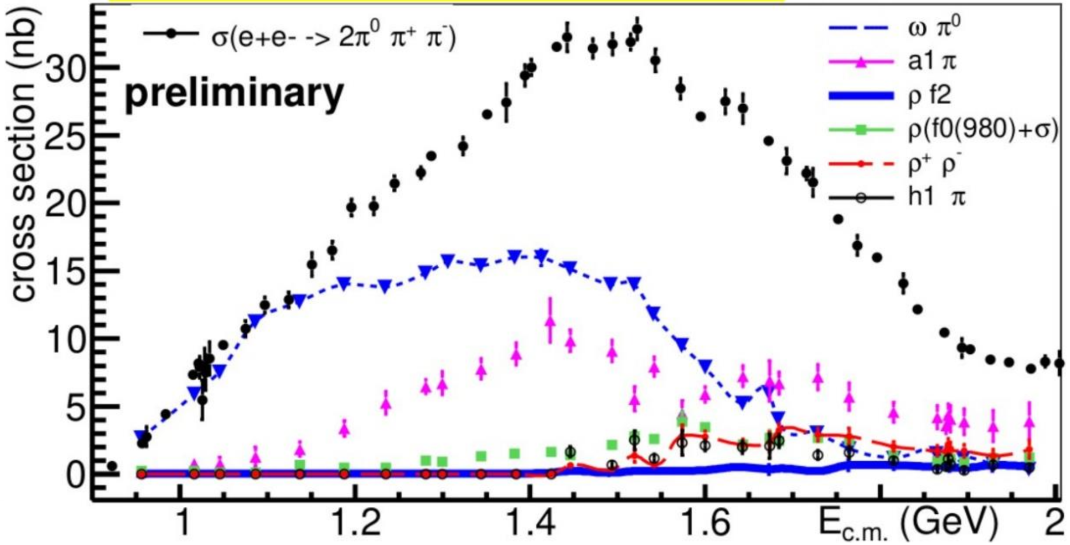

Intermediate resonances observed in data:

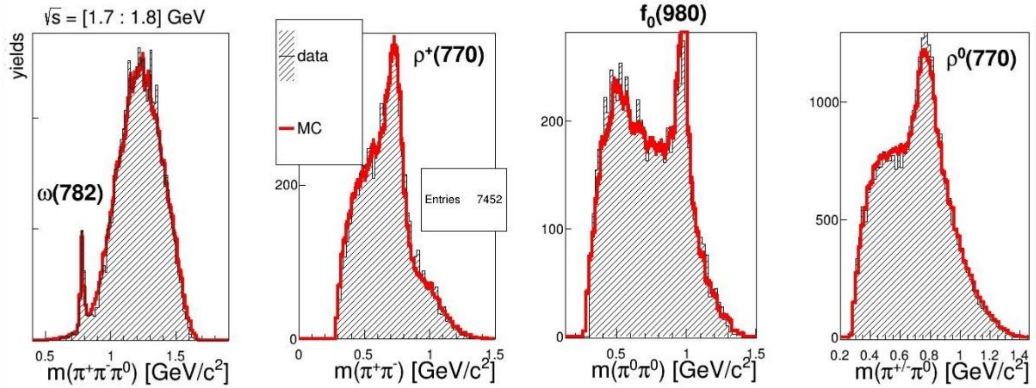

$R(s)$ at $N\bar{N}$ threshold

Detailed study of hadronic cross sections near $p\bar{p}$ and $n\bar{n}$ thresholds

2017 data

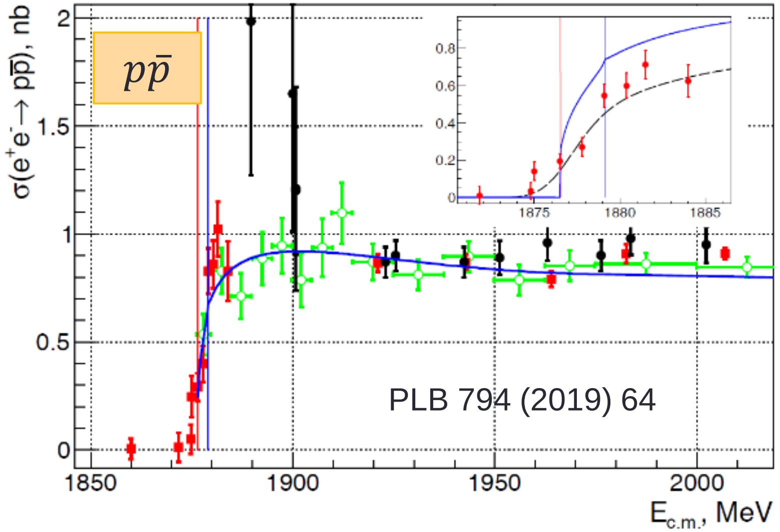

- sharp change in $e^+e^- \to p\bar{p}$, $3(\pi^+\pi^-)$, $K^+K^-\pi^+\pi^-$
- width ~1 MeV – consistent with energy resolution
- no structure in $e^+e^- \to 2(\pi^+\pi^-)$?

x5 more data in 2021, finer scan

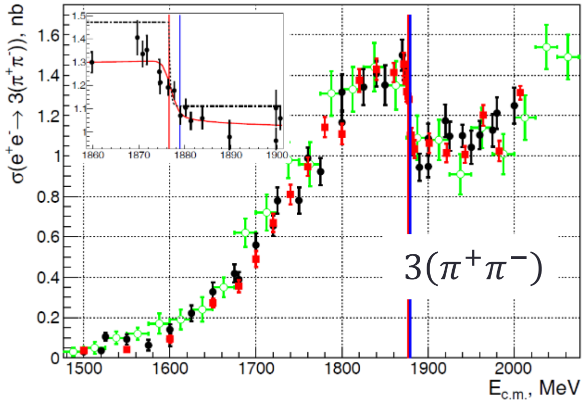

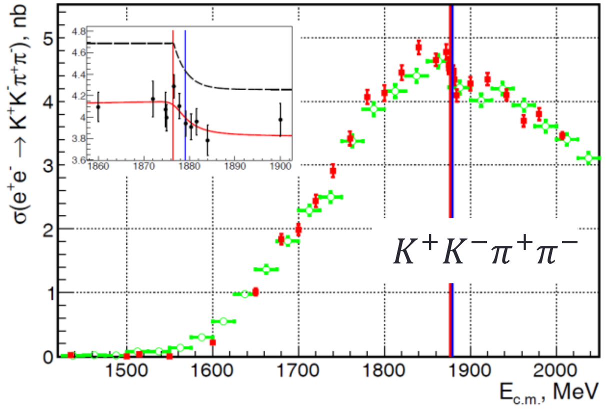

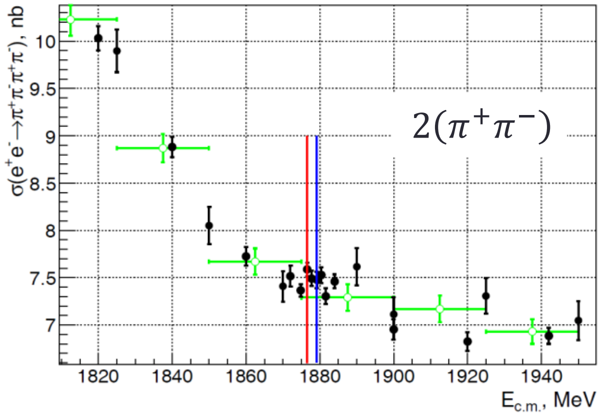

CMD-3 $e^+e^- \to \pi^+\pi^-$ analysis below 1 GeV

CMD-3 $e^+e^- \to \pi^+\pi^-$ analysis

Very simple kinematics, but the most challenging analysis due to high precision requirement: need to take into account many effects (which can affect result by 0.1% or more). High statistics is crucial!

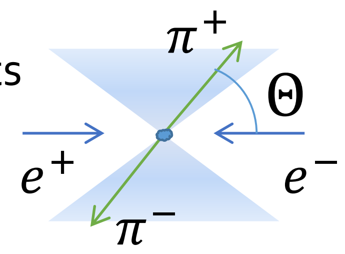

Main background: $e^+e^- \to e^+e^-, \mu^+\mu^-$

Measurement at CMD-3:

- several scans of the whole energy region below 2 GeV (took data in ρ energy region in 2013, 2018, 2020)
- employ correlations of the final particles: $e^+e^-, \mu^+\mu^-, \pi^+\pi^-$ separation either
  - by 2D momentum or
  - by 2D energy deposition

  independent measurements!
- many things to study: fiducial volume, pion decays, pions interactions in detector,backgrounds,...

P^- vs P^+ @$\sqrt{s} = 0.5$ GeV

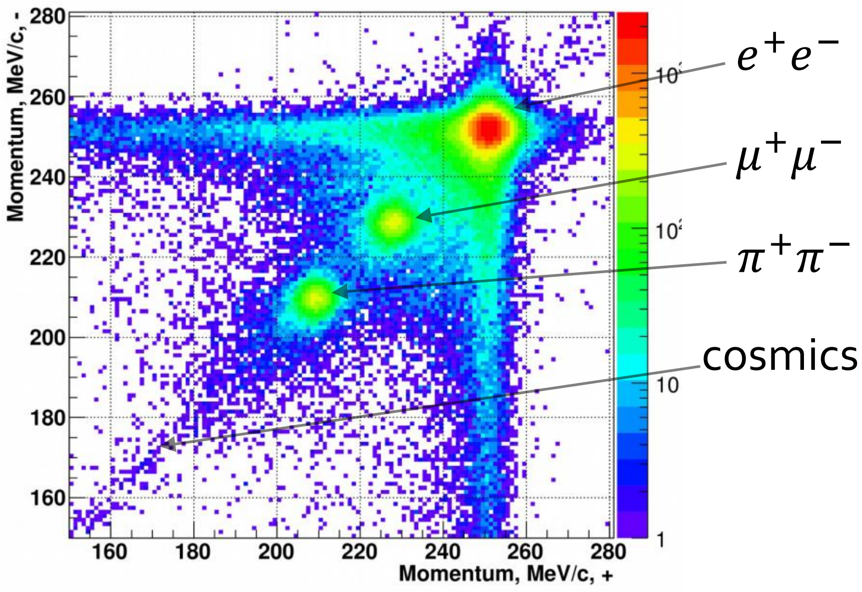

Three methods of separation of $e^+e^-, \mu^+\mu^-, \pi^+\pi^-$

Separation of $e^+e^-, \mu^+\mu^-, \pi^+\pi^-$ final states is based on binned likelihood minimization:

- using **energy deposition** (in LXe only)

$$-\ln L = -\sum_{bins} n_i \ln\left[\sum_{X=ee,\mu\mu,\pi\pi,bg} N_X f_X(E^+, E^-)\right] + \sum_X N_X$$

- using **momentum**

$$-\ln L = -\sum_{bins} n_i \ln\left[\sum_{X=ee,\mu\mu,\pi\pi,bg} N_X f_X(p^+, p^-)\right] + \sum_X N_X$$

$\pm$ sign reflects energy deposition and momentum of particle with corresponding charge

Independent method: by **angular distribution**

E^- vs E^+ @$\sqrt{s} = 0.78$ GeV

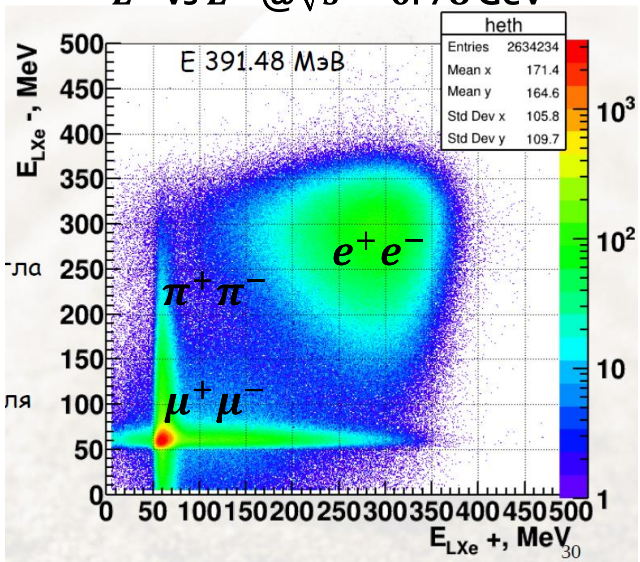

P^- vs P^+ @$\sqrt{s} = 0.5$ GeV

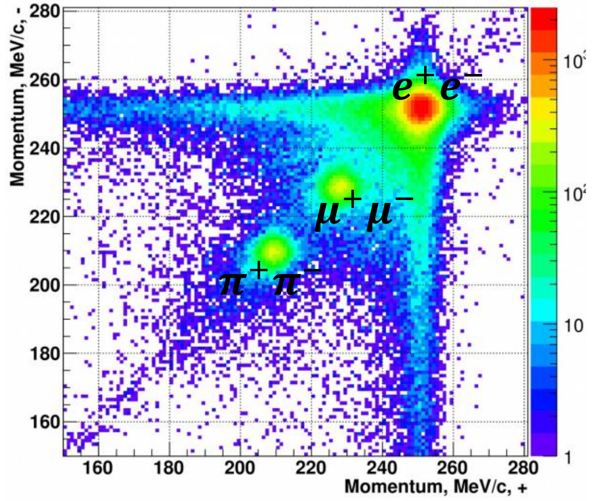

Where to get p.d.f.s $f_X(p^+,p^-)$ and $f_X(E^+,E^-)$?

Separation by momentum

PDFs are based on MC

- "Ideal" p.d.f.s are generated using $e^+e^- \to X^+X^-(\gamma)$ MC generator
- "Ideal" p.d.f.s are smeared with detector resolution function to get $f_X(p^+,p^-)$

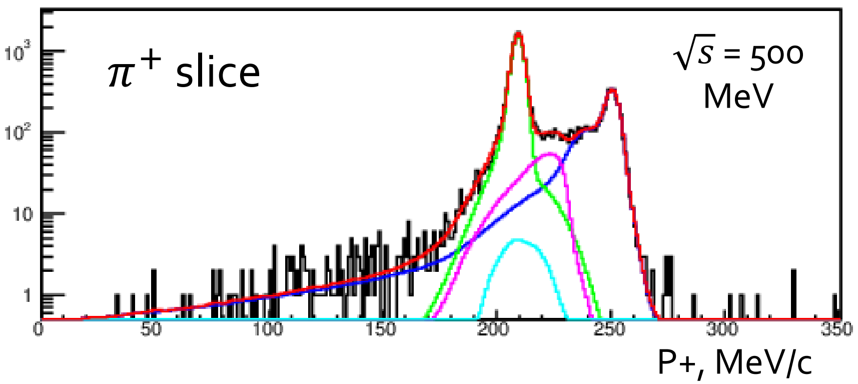

Separation by energy deposition

PDFs are mostly empirical

- $f_X(E^+,E^-)$ are partly constructed using the data:
  - tagged electrons and positrons
  - cosmic muons

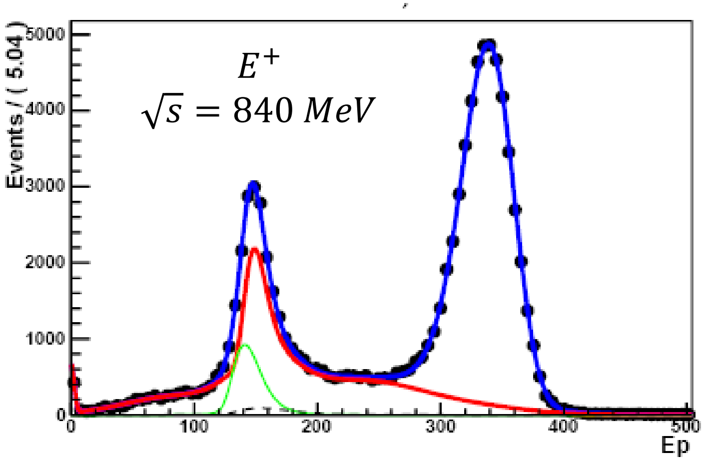

Comparison of various methods

By momentum:

$$N_{\pi\pi}/N_{ee} = 1.0187 \pm 0.0003$$

By energy:

$$\Delta\, N_{\pi\pi}/N_{ee} = +0.05\% \pm 0.033\%$$

By angular distribution:

- free asymmetry:

$$\Delta\, N_{\pi\pi}/N_{ee} = -0.23\% \pm 0.12\%$$

- fixed asymmetry:

$$\Delta\, N_{\pi\pi}/N_{ee} = +0.20\% \pm 0.08\%$$

Three methods agree to ~0.2%

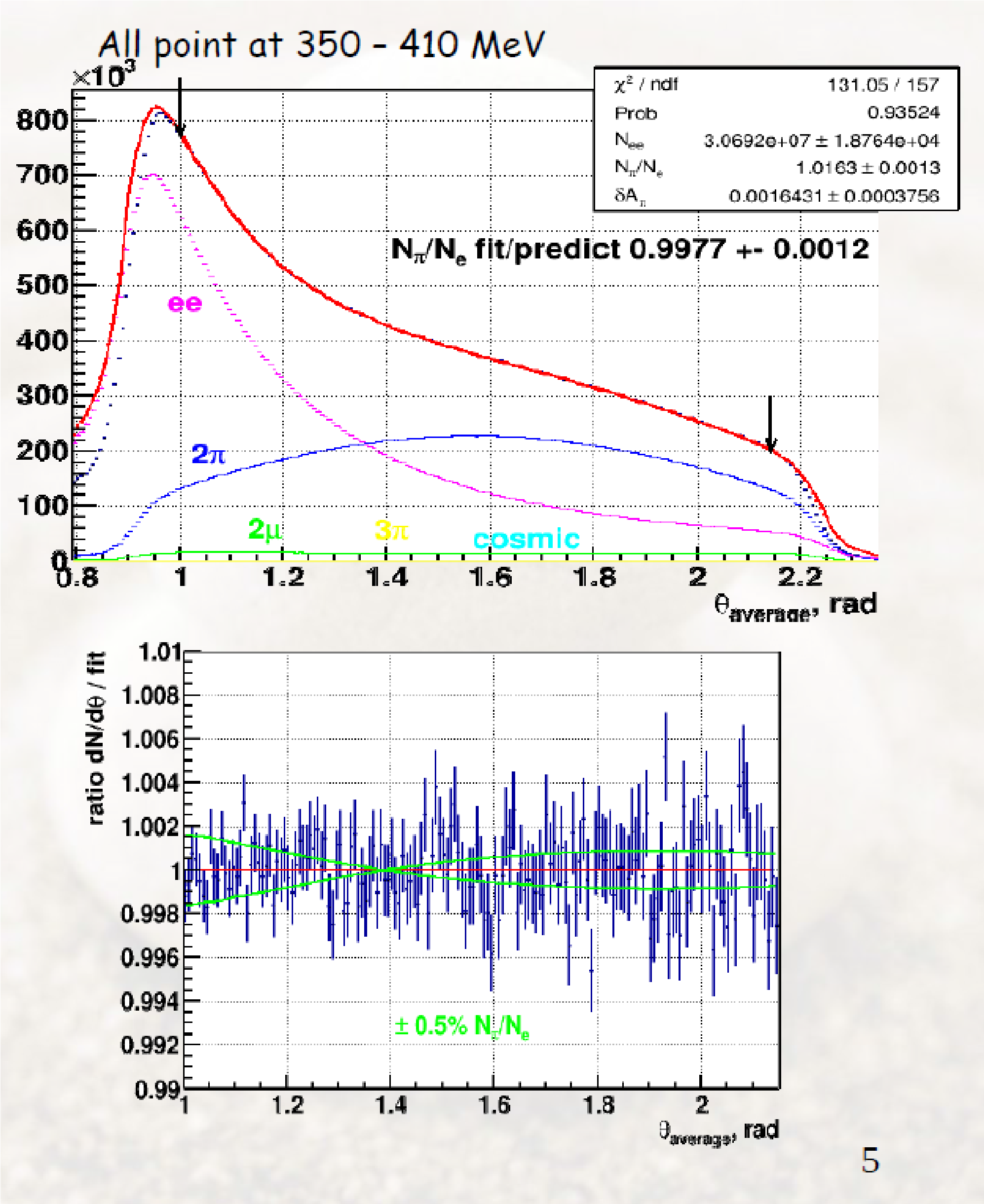

Fit of angular distribution

Efficiency corrections

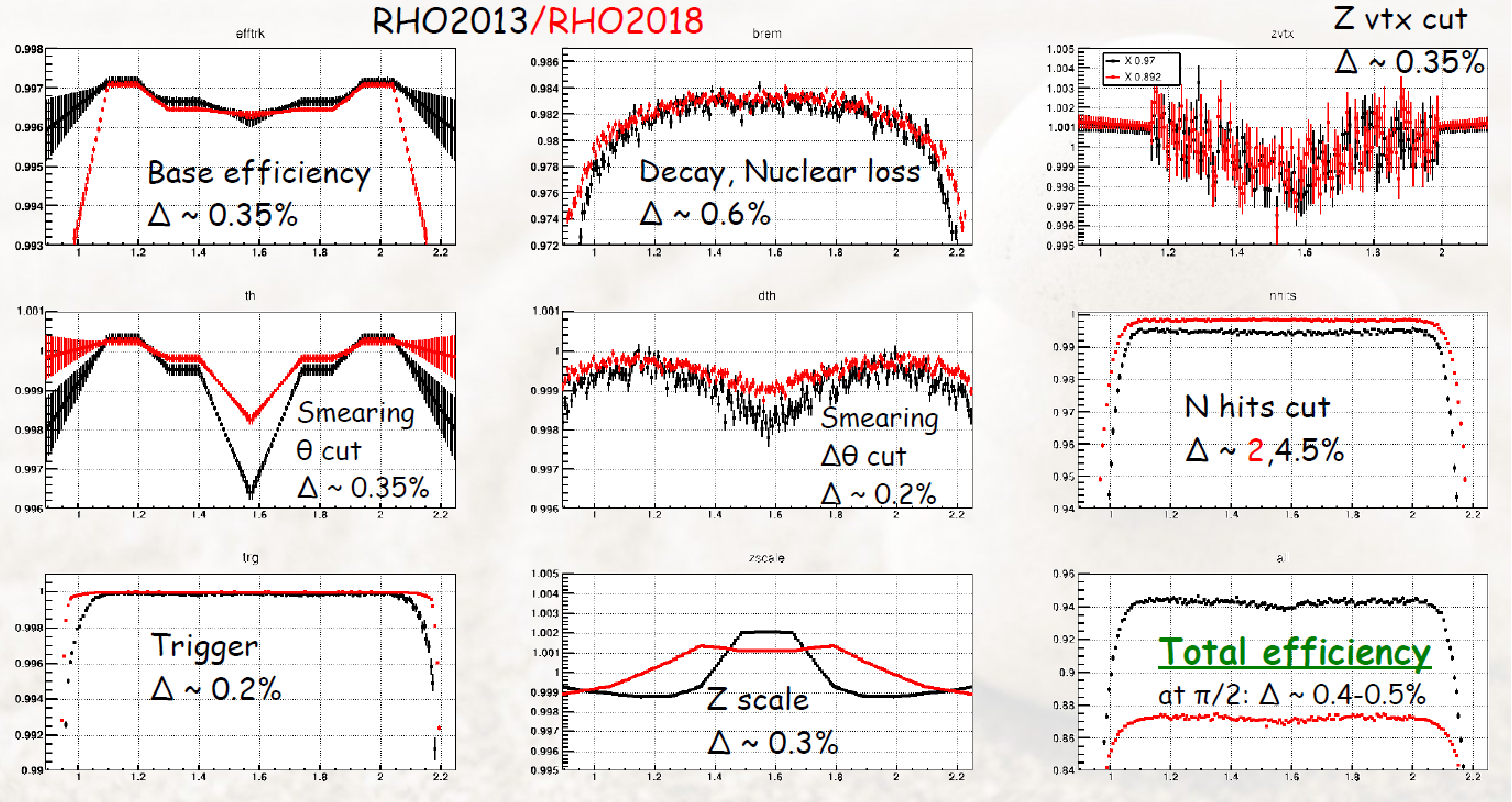

Difference between 2013 and 2018 data

2013 and 2018 data were taken in the same energy range, but with significantly different detector conditions:

- luminosity integral in 2018 is factor 2-5 larger
- data rate (luminosity) in 2018 was factor 2-5 larger
- drift chamber in 2013 operated without 4 middle layers (out of 19)
- Z-chamber (important for precision determination of fiducial volume) broke before 2018 run
- Z beam size in 2018 was twice wider
- calorimeter electronics was significantly updated before 2018

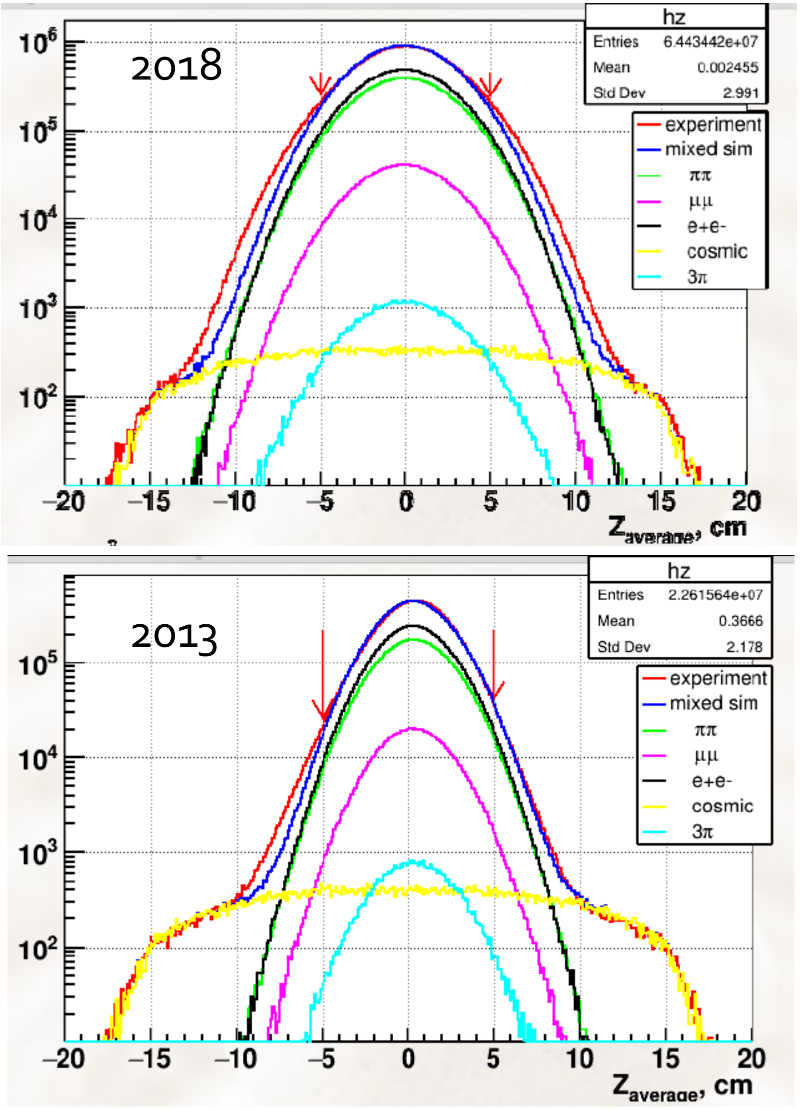

Z beam size

Dependance on theta cut

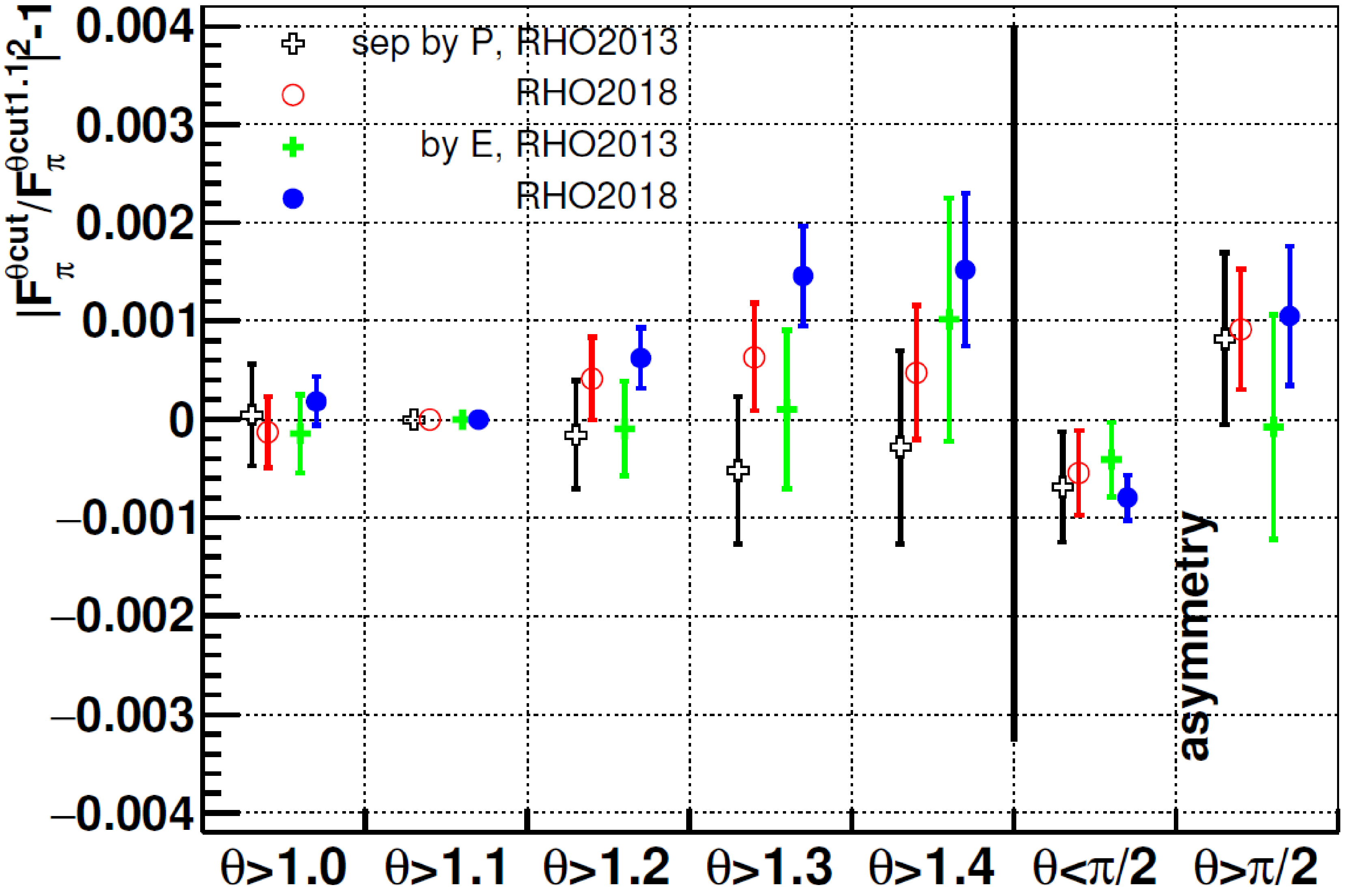

Charge asymmetry in $e^+e^- \to \pi^+\pi^-$

Charge asymmetry in $e^+\,e^- \to \pi^+\,\pi^-$ is due to interference between ISR/FSR and between one- and two-photon exchange

$$A = \left(N^{\pi}_{\Theta<\pi/2} - N^{\pi}_{\Theta>\pi/2}\right)/N$$

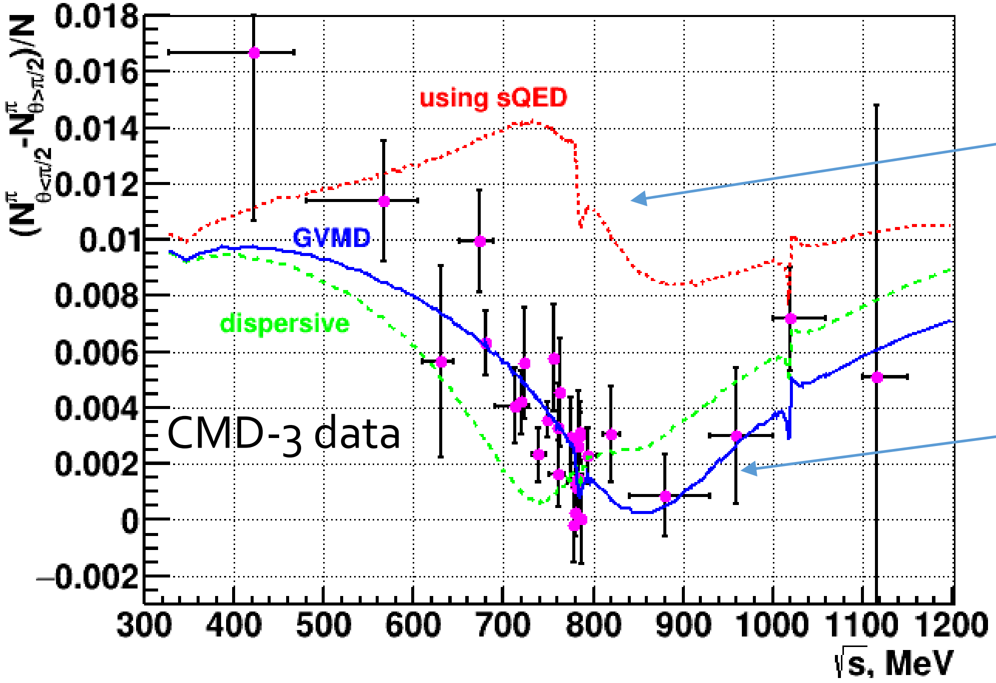

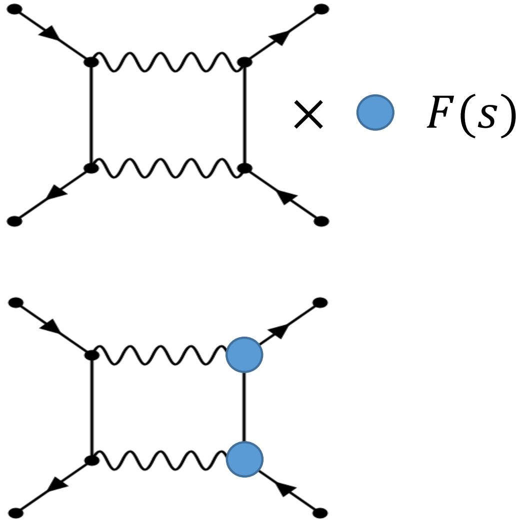

The theoretical model by Lee, Ignatov, PLB 833 (2022) 137283 (GVDM) describes well the CMD-3 data

Recent calculation in dispersive formalism Colangelo et al., JHEP 08 (2022) 295 confirms the effect. *Talk by Jacobo Ruiz de Elvira today.*

Internal checks

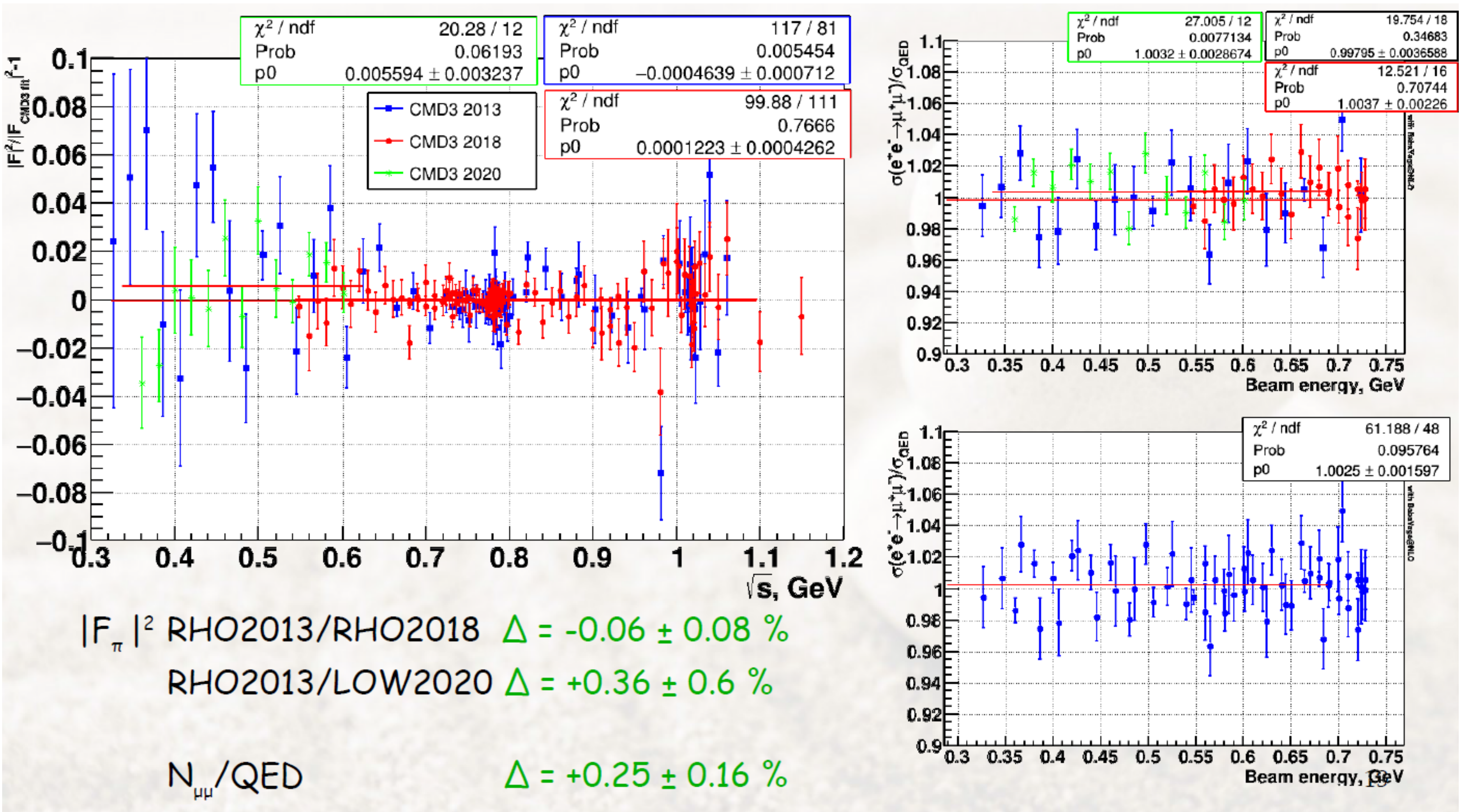

Comparison between different data sets

Comparison of measured $\sigma(e^+e^- \to \mu^+\mu^-)$ to QED

Radiative corrections

Measurement of $e^+e^- \to \pi^+\pi^-$ requires high precision calculation of radiative corrections.

We use two high-precision MC generators for $e^+e^- \to e^+e^-$:

- MCGPJ generator (0.2%)
- BaBaYaga@NLO (0.1%)

With high statistics we've observed inconsistencies in tails of distributions, which were traced to particulars of MCGPJ generator

After improvements, tails of e^+e^- spectra still differ by O(1-10%), which limits the precision

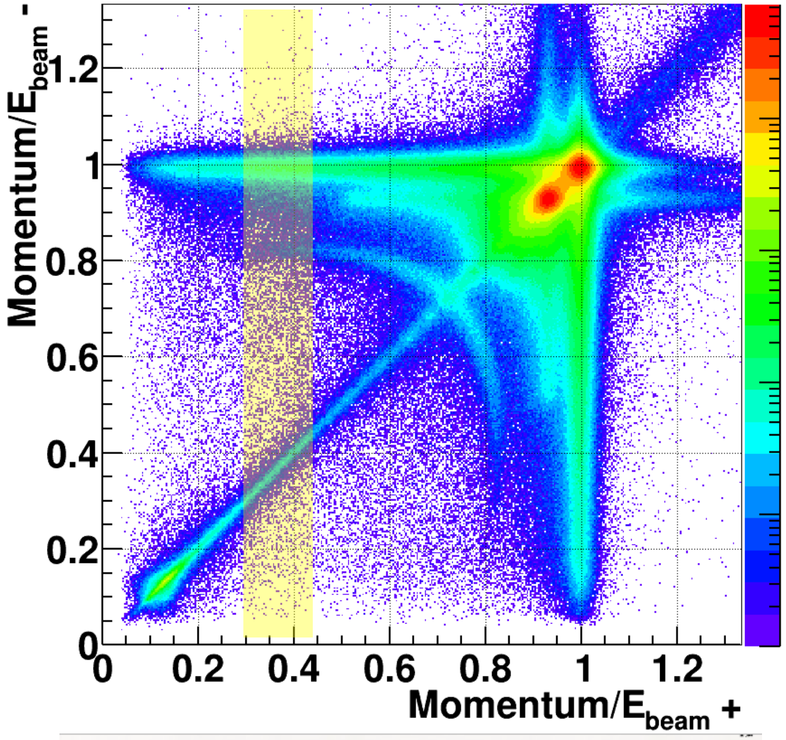

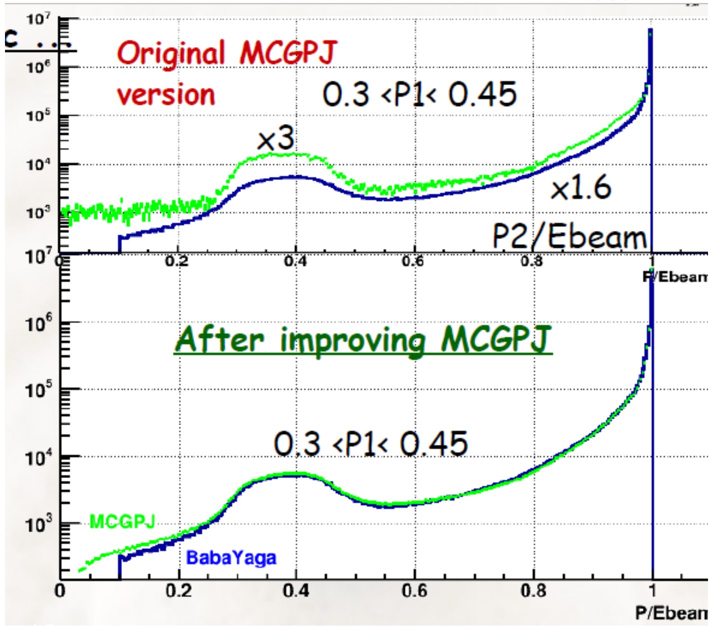

Radiative corrections

For the calculation of cross sections, there is very good agreement between MCGPJ and BaBaYaga@NLO.

But there is still some difference in spectra.

BaBaYaga@NLO shows better agreement with the data. We adopted it as the default MC generator for $e^+e^- \to e^+e^-$

Difference between spectra of MC generators leads to systematic error O(0.1%) (depends on energy)

NNLO MC generator for $e^+e^- \to e^+e^-$ is needed for higher precision

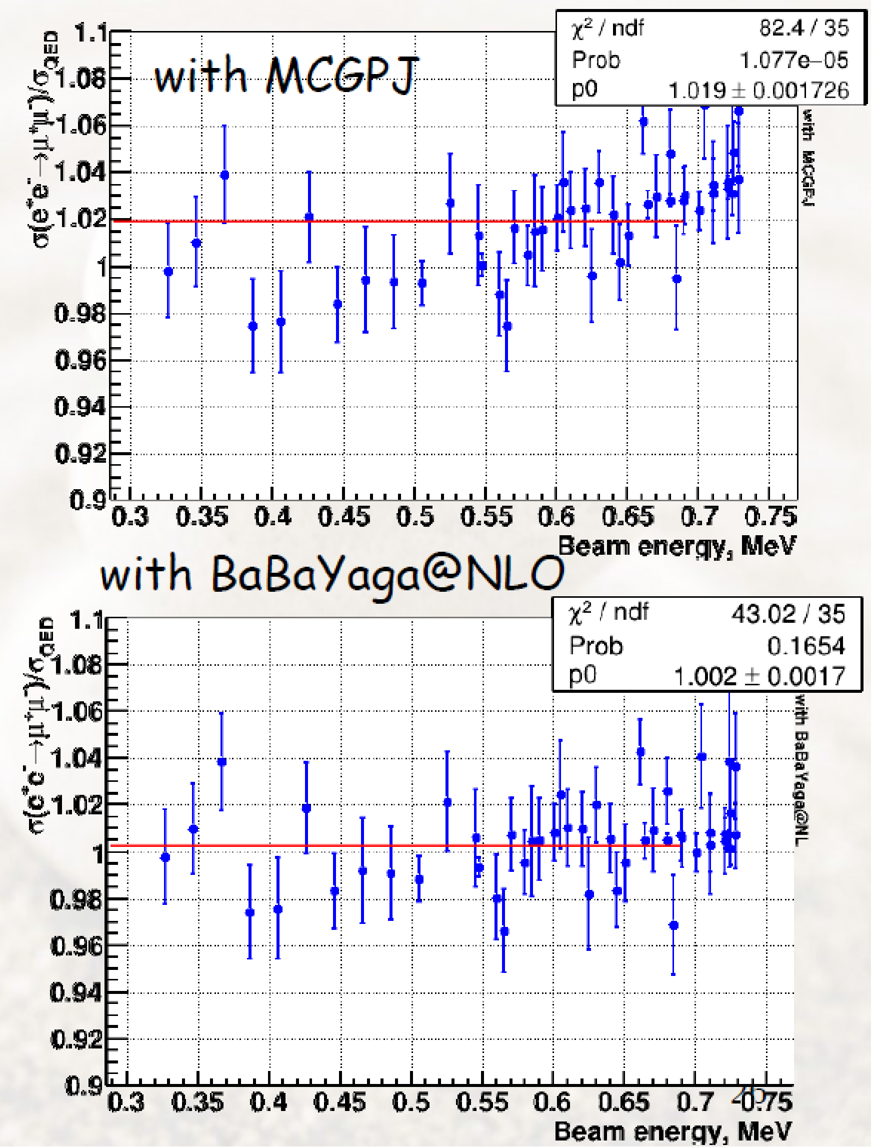

Comparison of measured and calculated $\sigma(e^+e^- \to \mu^+\mu^-)$ for different MC gen.

Statistical precision of CMD-3 data

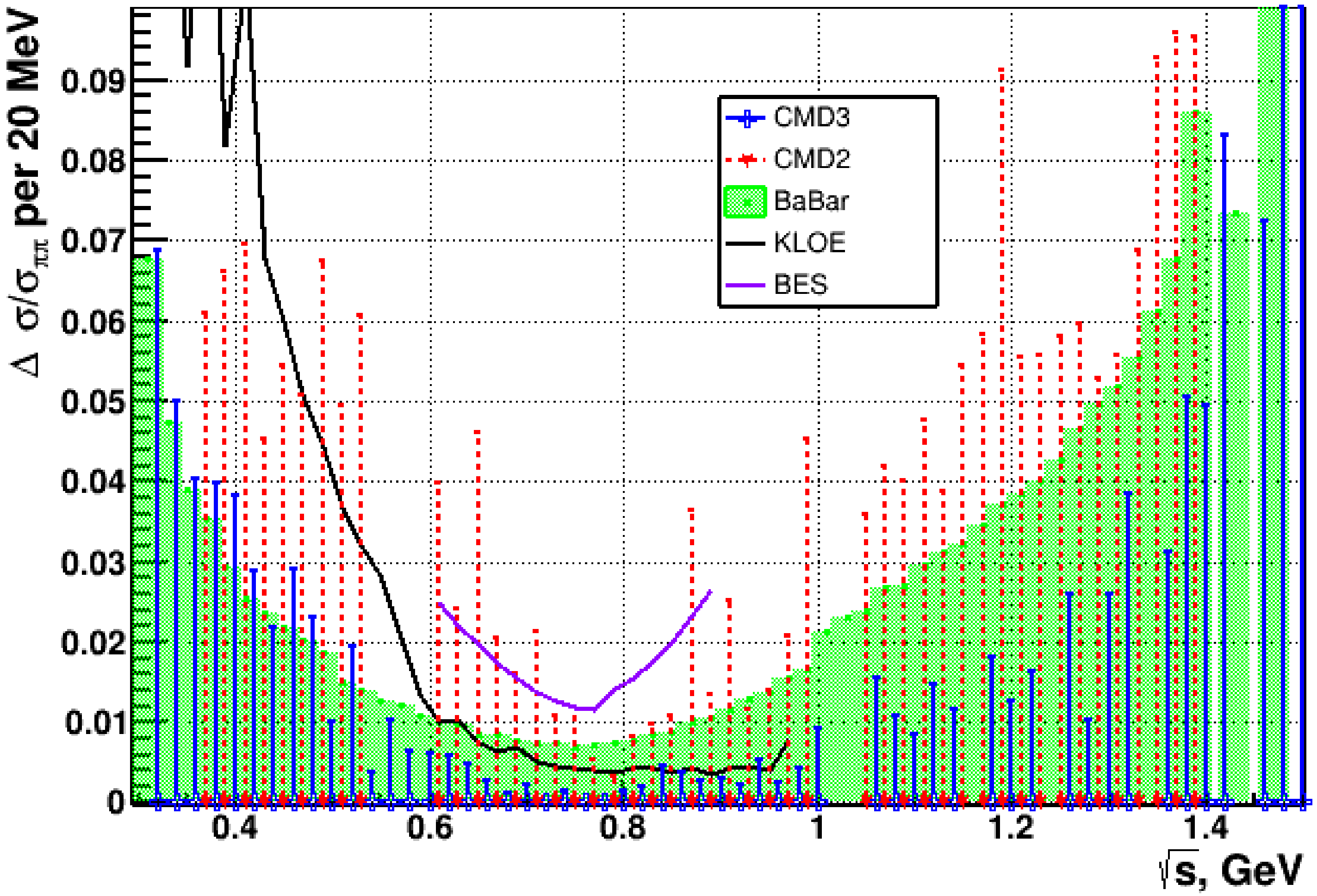

Relative statistical accuracy $\Delta\sigma/\sigma$ of various data sets in 20 MeV energy bins

The publication is in preparations. As soon as it ready, we'll announce results.

$e^+e^- \to \pi^+\pi^-$ at SND (2021)

First measurement of
$e^+e^- \to \pi^+\pi^-$
at VEPP-2000

The analysis is based on
4.7 pb^{-1} data recorded in 2013
(1/10 full SND data set)

π/e separation using ML (BDT)

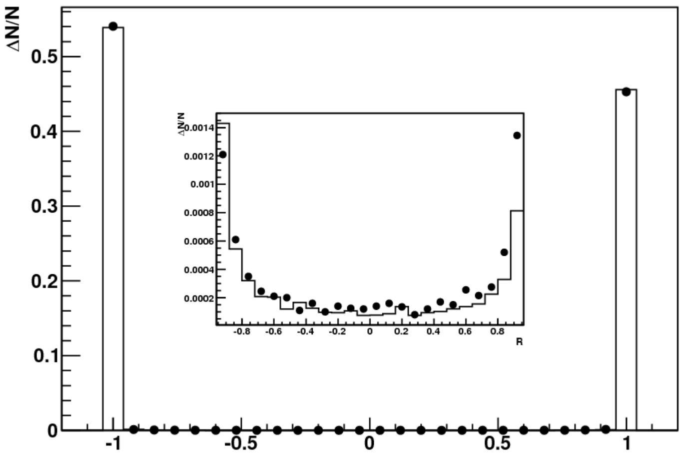

JHEP 2021,113 (2021)

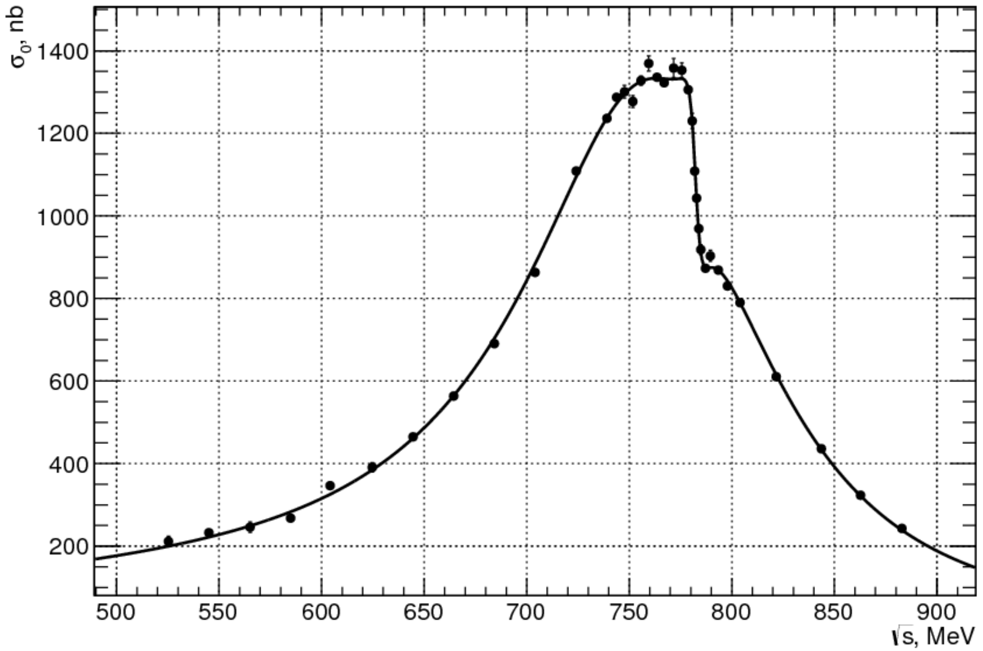

Systematic uncertainty on the cross section (%)

Source	< 0.6 GeV	0.6 - 0.9 GeV
Trigger	0.5	0.5
Selection criteria	0.6	0.6
e/π separation	0.5	0.1
Nucl. interaction	0.2	0.2
Theory	0.2	0.2
Total	**0.9**	**0.8**

$e^+e^- \to \pi^+\pi^-$ at SND (2021): comparison to other measurements

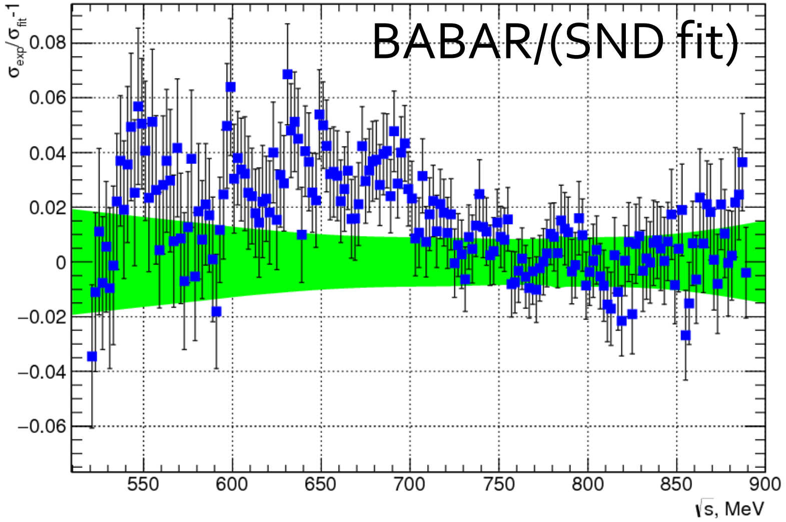

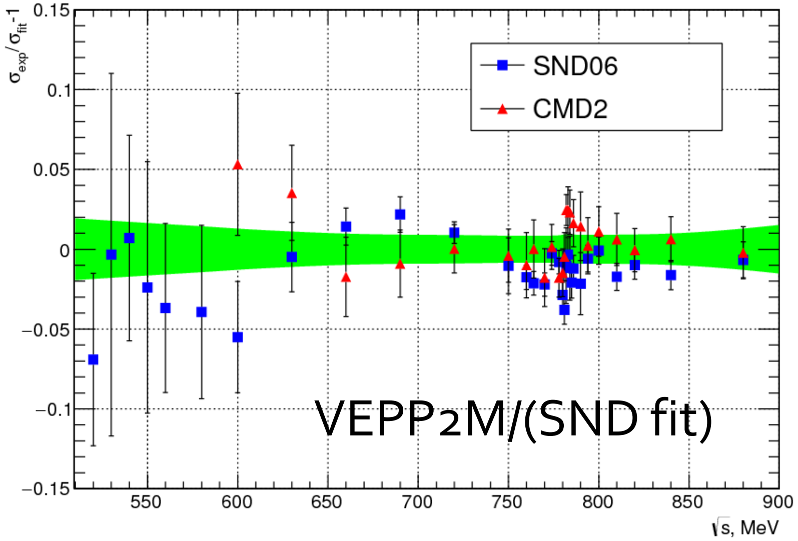

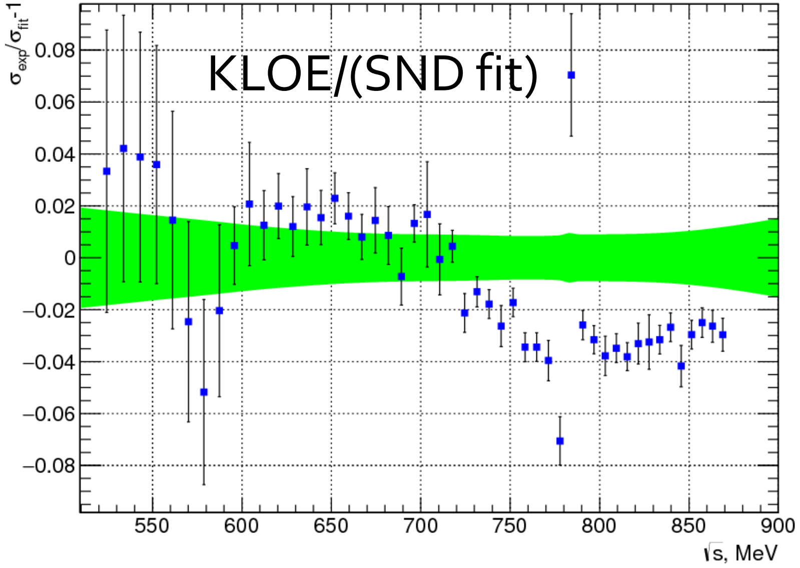

$0.53 < \sqrt{s} < 0.88$ GeV

	$a_\mu(\pi^+\pi^-) \times 10^{10}$
SND & VEPP-2000	$409.8 \pm 1.4 \pm 3.9$
SND & VEPP-2M	$406.5 \pm 1.7 \pm 5.3$
BABAR	$413.6 \pm 2.0 \pm 2.3$
KLOE	$403.4 \pm 0.7 \pm 2.5$

Summary

- VEPP-2000 collider is under operation, reached luminosity of $8 \cdot 10^{31}\ cm^{-2}s^{-1}$, 80% of design
- CMD-3 and SND detectors collected >600 1/pb each in the whole available energy range
- Data analysis is in progress, many result were published (mostly above 1 GeV)
- First pion formfactor data was published in 2021 by SND using ~10% of total available data set
- CMD-3 pion formfactor publication is under preparations; will be based on full data set
- The focus for near future is to collect record data set above 1 GeV